1

Light-responsive Surface: Photodeformable Cross-linked Liquid-Crystalline Polymers Based on Photochemical Phase Transition

Lang Qin and Yanlei Yu

Fudan University, Department of Materials Science, 220 Handan Road, Shanghai 200433, China

1.1 Introduction

Smart materials have drawn wide attention from physicists and chemists in recent years due to their superior properties. As a kind of novel material, smart materials have potential in applications in artificial muscles and soft actuators [1–5], biomedical systems [6], and so on. Among these smart materials, photodeformable materials promise significant roles in converting light energy into mechanical actuation. Compared to other stimulus-driven methods, such as by heat [7, 8], pressure [9], pH variations [10], electric field [11, 12], and magnetic field [13], light is a particularly ideal stimulus, since it is a clean energy and can be precisely and conveniently manipulated in terms of wavelength, intensity, and polarization direction. Besides, it is known that polymer matrix materials have many advantages, such as good flexibility, excellent corrosion resistance, high process ability, moderate mechanical strength, and light weight. Therefore, polymers that can undergo photoinduced deformation are utilized in many studies and definitely merit further investigation.

As a combination of cross-linked polymers and liquid crystals (LCs), cross-linked liquid-crystalline polymers (CLCPs) exhibit unique properties such as elasticity, anisotropy, stimuli-responsiveness, and molecular cooperation effect [14–16]. CLCPs, as three-dimensional networks, are able to undergo controllable and reversible shape change in response to an external stimulus. Since most of the CLCPs are chemically cross-linked, they are suitable to be used in a dry state. The incorporation of azobenzene chromophores into CLCPs can provide photoresponsiveness and induces a reduction in LC alignment and causes deformation upon exposure to UV light as a result of photochemical reaction of azobenzene units [16–18].

In this chapter, we mainly describe photoinduced deformation observed in azobenzene-containing CLCPs, focusing our attention on the factors affecting photodeformation, deformation forms, and light-driven soft actuators in both the macro- and microscale. The mechanism of deformation based on photochemical phase transition in CLCPs is also included. Our goal is to summarize the development of photoinduced behavior of CLCPs and provide an insight

Responsive Polymer Surfaces: Dynamics in Surface Topography, First Edition.
Edited by Danqing Liu and Dirk J. Broer.

into their potential applications as light-driven devices as well as on the recent progress in this field.

1.2 Photochemical Phase Transition

De Gennes proposed the possibility of using CLCPs as artificial muscles, by taking advantage of their substantial contraction in the direction of the director axis [19]. The basic principle behind the shape variation is the conformational change of the polymer backbone at LC-isotropic phase transition [20]. The polymer chains in an anisotropic LC environment deviate from the isotropic conformation. As a consequence, the coil-dimensions parallel and perpendicular to the LC director are different. If the CLCPs lose their anisotropic properties, which results from the decrease in alignment order of an LC, an isotropic chain conformation will be adopted and the whole sample will have to change its shape. For example, if the nematic CLCP films are heated toward the nematic–isotropic phase transition temperature, the nematic order will decrease, and when the phase temperature is exceeded, the CLCPs exhibit a general contraction along the alignment direction of the mesogens, and revert to their original size by expanding if the temperature is lowered back below the phase transition temperature. There have been a number of works on thermal-induced deformation of the CLCPs based on LC-isotropic phase transition ([21–25]). However, it would be expected that if the alignment of an LC can decrease by light, then this would be accompanied by equally dramatic mechanical responses.

Cooperative motion of molecules in LC phases may be most advantageous in changing the molecular alignment by external stimuli. The alignment of the majority of LC molecules will be changed if the alignment of a small portion of LC molecules is changed in response to an external stimulus. This phenomenon illustrates that LC molecules only require a small amount of energy to change the alignment: the energy needed to induce an alignment change of only 1 mol% of the LC molecules is enough to bring about the alignment change of the whole system. In other words, a huge amplification is possible in LC systems. When a small amount of a photo-chromic molecule is added into LCs and the resulting guest/host mixture is irradiated to cause photochemical reactions of the photochromic guest molecules, an LC-isotropic phase transition of the mixtures can be induced isothermally. Ikeda *et al.* reported the first explicit example of a nematic–isotropic phase transition induced by trans–cis photoisomerization of a nematic LC with an azobenzene guest molecule dispersed in it [25].

Azobenzene is a well-known chromophore that has two configurations. It undergoes trans to cis photoisomerization upon exposure to UV irradiation and irradiation with visible light leads to a cis to trans back-isomerization process. Therefore, azobenzene is the most frequently used photochromic moiety in photoresponsive polymers. The rod-like trans form of the azobenzenes stabilizes the phase structure of the LC phase, whereas its bent cis isomer tends to destabilize the phase structure of the mixture. As a consequence of two different conformations, the LC-isotropic phase transition temperature (T_c) of the mixture with the cis form (T_{cc}) is much lower than that with the trans

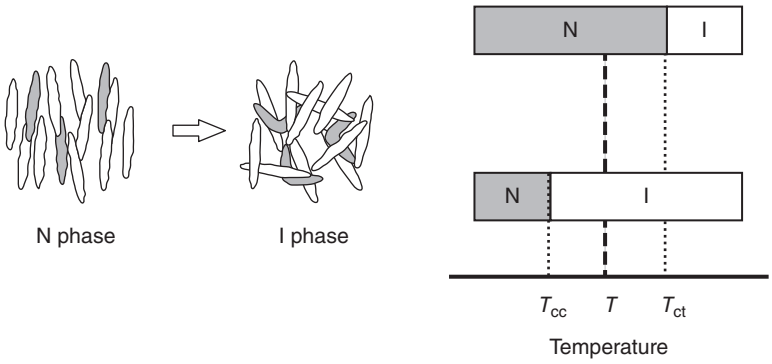

Figure 1.1 Phase diagrams of the photochemical phase transition of azobenzene/LC systems (N, nematic; I, isotropic). (Ikeda 2003 [26]. Reproduced with permission of Royal Society of Chemistry.)

form (T_{ct}). If the temperature of the sample (T) is between T_{ct} and T_{cc} and the sample is irradiated to cause trans–cis photoisomerization of the azobenzene guest molecules, T_c decreases because of the increase of the cis form. When T_c becomes lower than the irradiation temperature T, LC-isotropic phase transition of the sample is induced. The sample reverts to the initial LC phase through cis–trans back-isomerization due to reversible photochromic reactions. Thus, phase transitions of LC systems can be induced isothermally and reversibly by photochemical reactions of photoresponsive guest molecules (Figure 1.1) [26].

Ikeda *et al.* reported the first example of the photochemical phase transition in liquid-crystalline polymer (LCP)s [27–29]. They demonstrated that by irradiation of LC polymers doped with low-molecular-weight azobenzene derivatives with UV light to give rise to trans–cis isomerization led to a nematic–isotropic phase transition; upon cis–trans back-isomerization, the LCPs reverted to the initial nematic phase. Although doping the chromophores in a matrix is most convenient, the resultant LCP systems often exhibit instabilities, such as phase separation and microcrystallization. This occurs because of the mobility of the azobenzene chromophores in the matrix and the propensity of the dipolar azobenzene units to form aggregates. In order to address the problem, higher quality LCP systems are obtained when the azobenzene moiety is covalently bound to the host polymer matrix (Figure 1.2). The azobenzene moiety plays a role both as a mesogen and a photosensitive group in azobenzene derivatives that form an LC phase.

1.3 Photodeformation

1.3.1 Photoinduced Contraction and Expansion

Finkelmann *et al.* reported pioneering work on photodeformation of a monodomain nematic CLCP, which had a polysiloxane main chain and azobenzene chromophores at cross-links. The CLCP film generated a

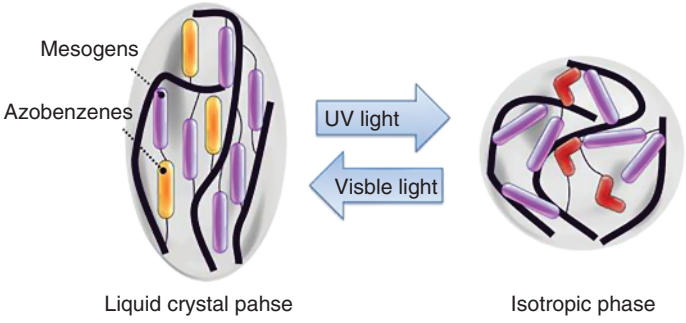

Figure 1.2 Schematic illustration of reversible LC-isotropic photochemical phase transition. (Wei and Yu 2012 [3]. Reproduced with permission of Chinese Physical Society.)

contraction by 20% upon irradiation with UV light to give rise to the trans–cis isomerization of the azobenzene moieties (Figure 1.3) [21]. It is necessary to take photomechanical effects into consideration: the subtle variation in nematic order upon trans–cis isomerization causes a significant uniaxial deformation of the LCs along the director axis when the LC molecules are strongly associated by covalent cross-linking to form a three-dimensional polymer network. The contracted elastomer thermally returned to the original state due to the cis–trans back-isomerization after stopping irradiation. Terentjev *et al.* prepared CLCPs with a wide range of azobenzene derivatives as photoresponsive moieties and examined the deformation behavior of CLCPs upon exposure to UV light [30, 31].

Keller and coworkers synthesized oriented monodomain nematic side-on CLCPs containing azobenzenes (Components **2a,b**) by photopolymerization with a near-infrared photoinitiator [32]. The photopolymerization was performed with aligned azobenzene monomers in conventional LC cells. The obtained thin films were found to show fast (<1 min) photochemical contraction of up to 18% upon exposure to UV light and a slow thermal recovering in the dark (Figure 1.4).

1.3.2 Photoinduced Bending Movements

In order to observe a strong effect of the isomerization, high concentrations of the photoresponsive molecules are required. This will lead to a high optical density of photoresponsive molecule-containing film. The light absorption intensity within the film is no longer constant, and the extent of isomerization varies throughout the sample. Due to the different degrees of elongation or contraction, the internal stress can lead to strong bending deformation (Figure 1.5). Furthermore, the azobenzene moieties are preferentially aligned along the rubbing direction of the alignment layers, and thus the decrease in the alignment order of the azobenzene moieties is produced along this direction, which contributes to the anisotropic bending behavior.

Ikeda and coworkers were the first to report the photoinduced bending behavior of macroscopic CLCPs containing azobenzene [33]. Compared to the two-dimensional contraction or expansion, the bending mode, three-dimensional movement, can be advantageous for a variety of real

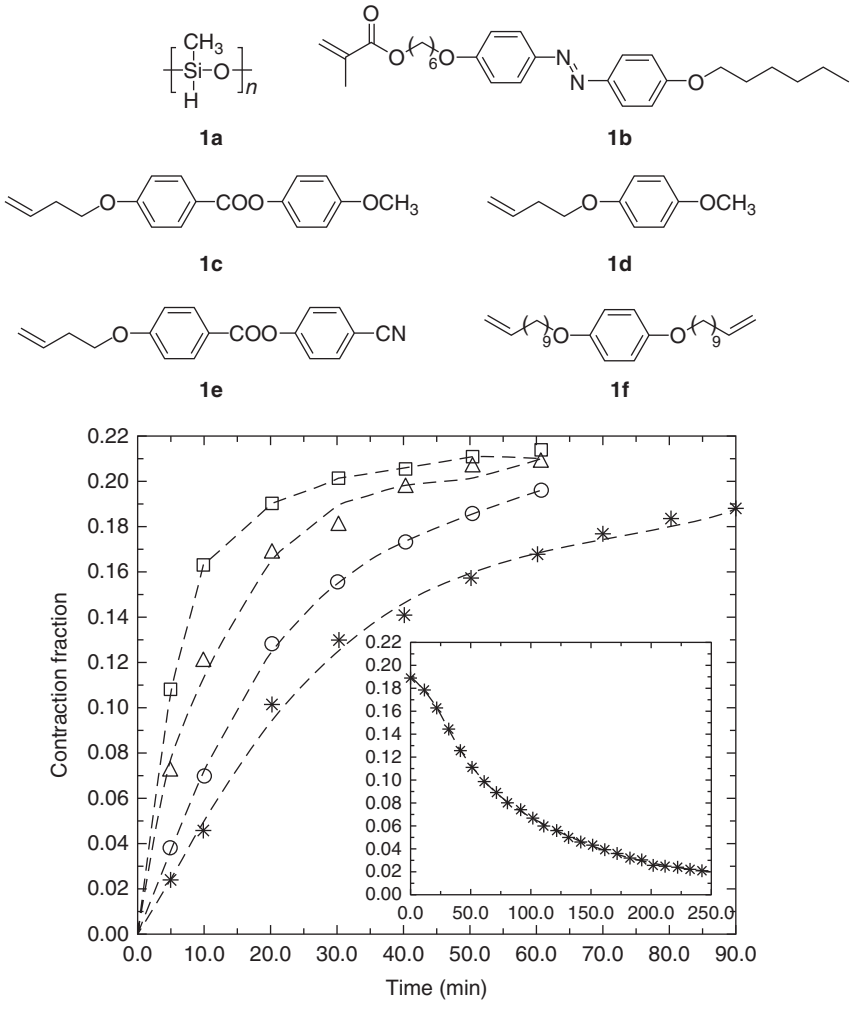

Figure 1.3 Photo-induced contraction of CLCP prepared from **1a–f**. □ = 313 K, Δ = 308 K, ○ = 303 K, * = 298 K. (Inset) Recovery of the contracted CLCP at 298 K after irradiation was switched off. (Finkelmann 1987 [14]. Reproduced with permission of Wiley.)

manipulation applications. The monodomain CLCP film bent toward the irradiation source along the rubbing direction and reverted to the initial flat state upon exposure to visible light. This bending and unbending behavior was reversible and controlled by simply altering the wavelength of the incident light. Furthermore, when the film was rotated by 90°, the bending behavior was again observed along the rubbing direction. These results illustrate that the bending is anisotropically induced and occurs only along the rubbing direction.

Ikeda and coworkers prepared the films by thermal polymerization of a liquid-crystal monomer **3a** and a diacrylate cross-linker **3b**. By means of selective absorption of linearly polarized UV light in polydomain CLCP films, they succeeded in controlling the direction of photoinduced bending so that a single

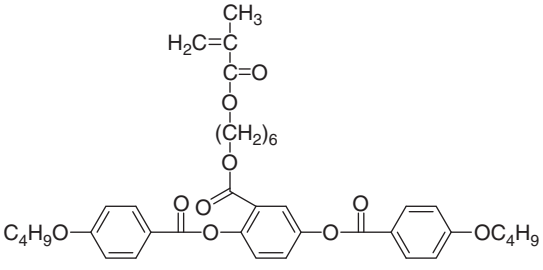

2a

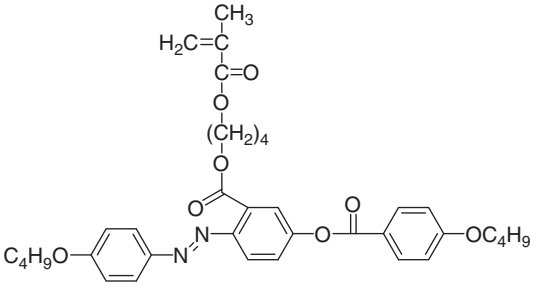

2b

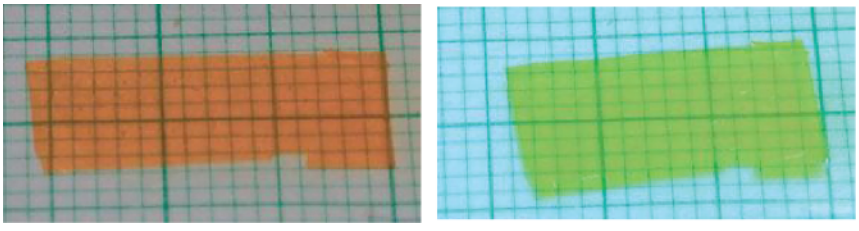

(a) (b)

Figure 1.4 Photographs of photodeformation of azobenzene side-on CLCP (a) before irradiation and (b) under irradiation with UV light. (Iqbal 2013 http://www.mdpi.com/1996-1944/6/1/116/htm. Used under CC BY 3.0 license https://creativecommons.org/licenses/by/3.0/.)

polydomain CLCP film was found to be bent repeatedly and precisely along any chosen direction (Figure 1.6a) [34]. The film bent toward the irradiation source in a direction parallel to the polarization of the light and completely reverted to its initial flat state upon exposure to visible light with a wavelength longer than 540 nm. The polydomain CLCP film consists of many micro-sized domains of azobenzene moieties aligned in one direction in each domain. Although macroscopically the direction of alignment is random (Figure 1.6b), upon exposure of the film to linearly polarized light, the selective absorption of light in a specific direction leads to a contraction in specific domains where the azobenzene moieties are aligned along the direction of light polarization.

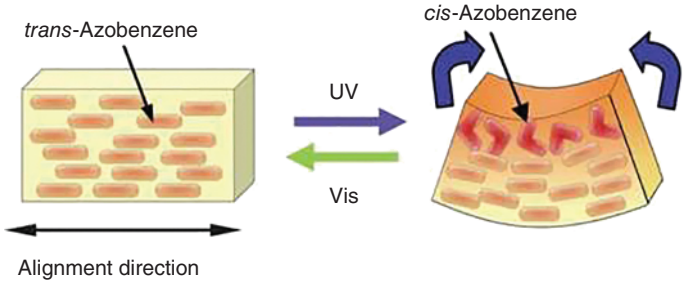

Figure 1.5 Plausible mechanism of the photoinduced bending of CLCP film. (Zhang *et al*. 2010 [49]. Reproduced with permission of Royal Society of Chemistry.)

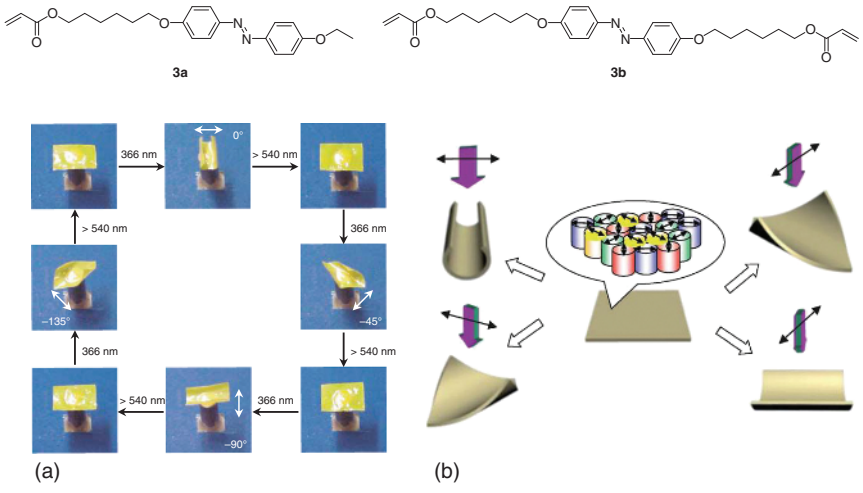

Figure 1.6 (a) Precise control of the bending direction of a film by linearly polarized light: photographs of the polydomain film in different directions in response to irradiation by linearly polarized light at different angles of polarization (white arrows) at $\lambda = 366$ nm; the bent films are flattened by irradiation with visible light at $\lambda > 540$ nm. (b) Schematic illustration of the plausible bending mechanism. (Zhang *et al*. 2010 [49]. Reproduced with permission of Royal Society of Chemistry.)

Chemical cross-linking is not the only route to fabricate CLCP films. Ikeda and coworkers prepared hydrogen-bond CLCP films using two cross-linkers (Components **4a,b**) capable of recognizing hydrogen bond donor molecules at the pyridyl ends [35]. A complex of a copolymer (**4c**), which has both carboxyl groups and azobenzene moieties, and the cross-linker was obtained from a tetrahydrofuran solution; then the melt complex was sandwiched between two sodium chloride plates with rubbing treatment to prepare hydrogen-bonded CLCP films. It was observed that the film without the azobenzene group in the cross-links showed no deformation on exposure to UV light, whereas the film with azobenzene cross-links bent toward the actinic light source along the alignment direction of the mesogens. Their photoinduced bending and unbending behaviors are similar to that of the covalently bonded CLCP films. These illustrate

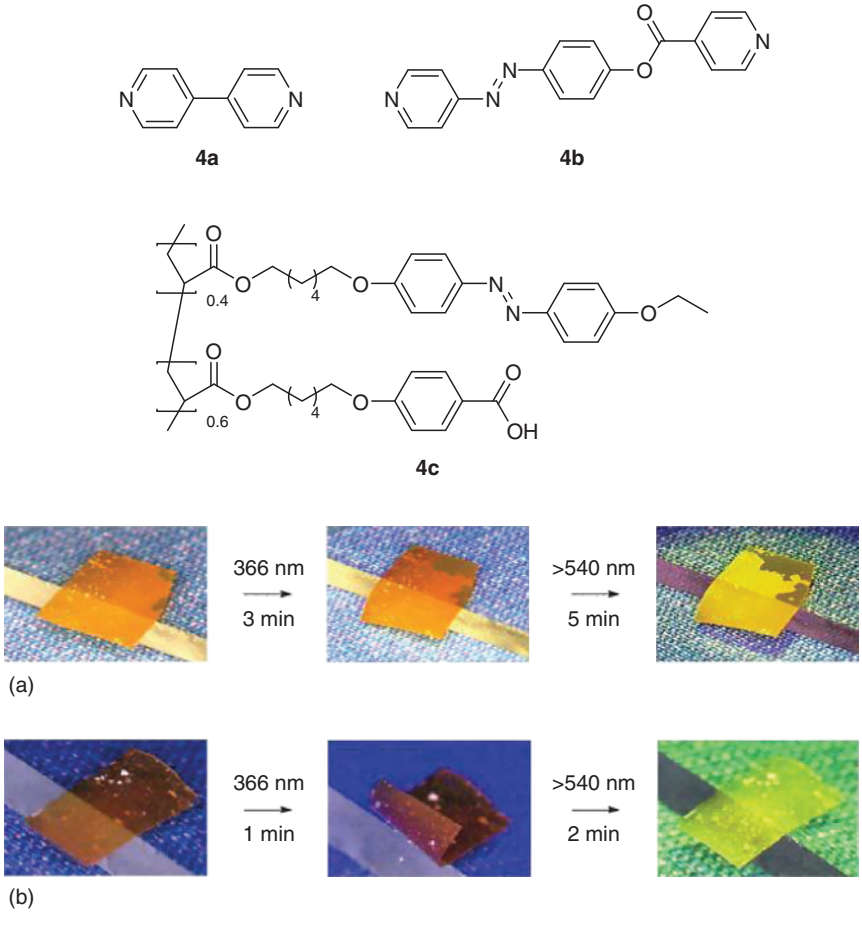

Figure 1.7 Photoresponsive behavior of the hydrogen-bonded CLCP films of (a) **4a** + **4c** and (b) **4b** + **4c**. (Mamiya *et al*. 2008 [35]. Reproduced with permission of Royal Society of Chemistry.)

that the cross-links formed by hydrogen bonds can convert the motion of the mesogens into a macroscopic change of the CLCP films. This kind of supramolecularly self-assembled CLCP films were reconstructed through cross-linking and decross-linking of the hydrogen bonds, and make the photoinduced bending of reformed CLCP films induced repeatedly, which is superior to the covalently bonded polymers (Figure 1.7). Lee and coworkers first reported a novel main-chain photochromic LCP without any chemical cross-linking, which exhibited excellent 3D bending behavior at room temperature [36]. Due to the lack of chemical cross-linking in the LCP, it was possible to process the polymer into any shape of film by solution casting. The bending of the film could be precisely controlled in various directions by polarized UV light at room temperature.

Furthermore, Ikeda *et al.* fabricated the thin cross-linked azobenzene LCP films with an adhesive-free bilayer structure by one-step electron beams (EBs)

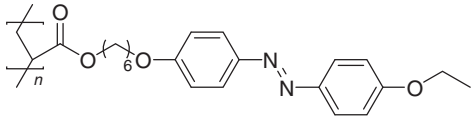

5

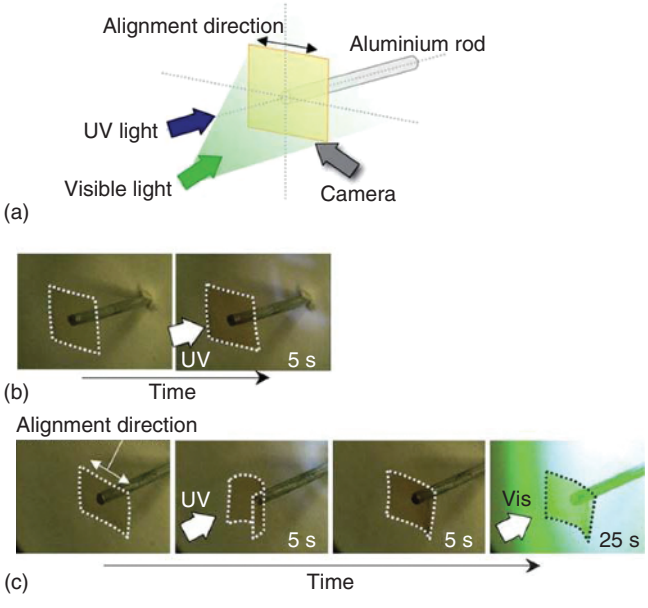

Figure 1.8 Photoresponsive behavior of EB-cross-linked Components **5**/PE bilayer films upon irradiation with UV (220 mW cm^{-2}) and visible (50 mW cm^{-2}) light at room temperature. (a) Schematic illustration of the experimental setup; (b) photoresponsive behavior of bilayer film prepared by EB irradiation at a dose of 0.5 MGy; (c) photoinduced bending behavior of the film prepared by EB irradiation at a dose of 10 MGy. Film size: 5 mm × 4 mm; thickness of the bilayer film: 25 μm (PE) and 2.5 μm (Components **5**). (Naka *et al*. 2011 [37]. Reproduced with permission of Royal Society of Chemistry.)

irradiation (Figure 1.8) [37]. The polyethylene (PE) substrates were coated with linear azobenzene LCPs (Components **5**), and subsequently the azobenzene layers were cross-linked by irradiation with electron beams. When the bilayer films were irradiated from the side of the azobenzene layer, they bent toward the actinic light source, while upon UV irradiation from the side of the polyethylene layer they bent away from the actinic light source. The bent films reverted to the initial flat state when the light turned off. These processes could be repeated at room temperature.

It is well known that human skeletal muscles are composed of many bundles of fibers and their crucial function is to convert chemical energy into mechanical work. Ikeda *et al.* prepared CLCP fibers containing an azobenzene moiety by two-step reactions [38]. It was found that the CLCP fibers exhibited a T_g of around 60 °C and showed a high order of mesogens along the fiber axis. When

the CLCP fiber was irradiated with UV light, the CLCP fiber bent toward the actinic light source along the fiber axis. The bent fiber recovered to the initial state upon exposure to visible light. The photoinduced bending and unbending of the CLCP fiber was reversible simply by changing the wavelength of the actinic light, similar to that of CLCP films. Furthermore, a three-dimensional control of bending direction in the CLCP fibers was carried out with the experimental setup shown in Figure 1.9. Since the shape of the CLCP fiber was approximately cylindrical, the direction of the bending could be controlled by changing the irradiation direction of the actinic light. The generated stress upon contraction of the natural surface length reached 210 kPa, which is similar to the stress in human muscles (around 300 kPa).

Recently, Zhang and coworkers synthesized a series of an azobenzene main-chain LCPs by Michael addition reaction under mild reaction conditions [39]. Supramolecular hydrogen-bonding CLCP fibers were directly fabricated by using the simple melt spinning method, but in the absence of any chemical cross-linker, which was proved to have a high order of mesogens along the fiber axis. As shown in Figure 1.10, the bending and unbending of the fibers were fast and reversible and could be easily controlled by changing the wavelength of the incident light. The reversible deformation of the fibers was found to repeat over 100 cycles.

In order to achieve the orientation in the CLCP films, generally, an aligned polyimide layer with parallel grooves generated by mechanical rubbing along one direction was often used to orient the LC molecules. Lately, by using highly aligned carbon nanotube (CNT) sheets, a new and general method to prepare photodeformable CLCP/CNT nanocomposite films was developed [40]. The CLCP/CNT composite film exhibited a rapid and reversible deformation under alternate irradiation by UV and visible light (Figure 1.11). This actuation is derived from the structure change in the composite film, which results from the photoisomerization of the azobenzene moieties. Compared to the CLCPs prepared by the conventional mechanical rubbing method, the introduction of aligned CNTs remarkably improved mechanical strength and high electrical conductivity of the CLCP film.

1.3.3 Photoinduced Twisting Movements

Besides the bending behavior, the coiling movement of CLCPs in response to light was also reported. Broer and coworkers prepared CLCP films with a densely cross-linked, twisted configuration of azobenzene units as shown in Figure 1.12 [41]. Although the networks were stiff and glassy at room temperature, the films showed large-amplitude coiling motion as well as bending motion upon exposure to UV light, which was based on the configuration of twisted LC alignment of 90°.

Recently, Iamsaard and coworkers reported complex motion of spring-like CLCP materials [42]. Chiral dopants **9a** and **9b** were added to the liquid-crystalline mixture to induce a left-handed and right-handed twist in LC, respectively. The film had a twisted geometry, in which the orientation of the LC director changes smoothly by 90° from the bottom surface to the top surface. The films coiled spontaneously into spring once they were cut into ribbons. Under

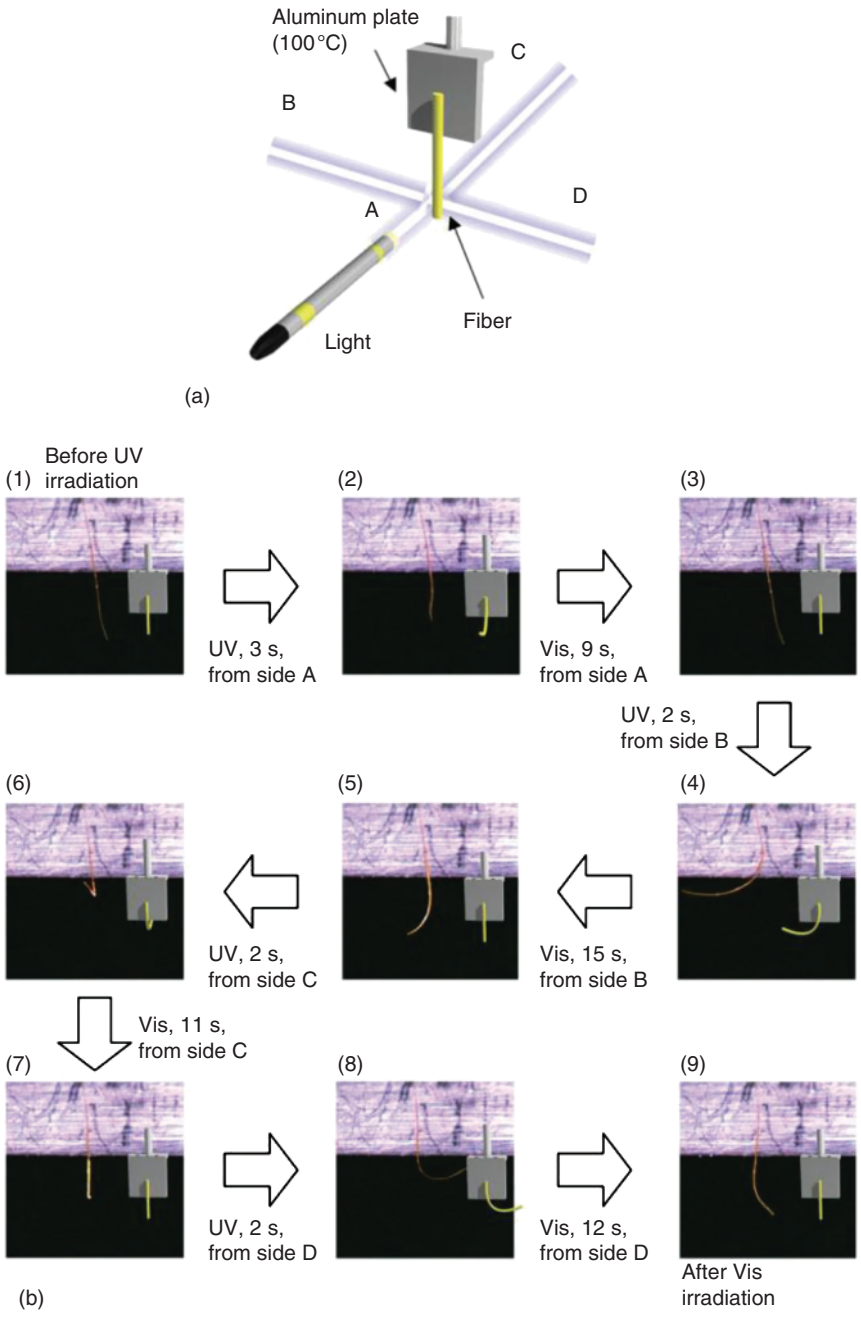

Figure 1.9 (a) Schematic illustration of experimental setup. (b) Photographs of the CLCP fiber that exhibits photoinduced bending and unbending behavior upon irradiation with UV light (100 mW cm^{-2}) and visible light (120 mW cm^{-2}). The inset of each photograph is a schematic illustration of the state of the fiber. The size of the fiber is 30 mm × 20 μm.

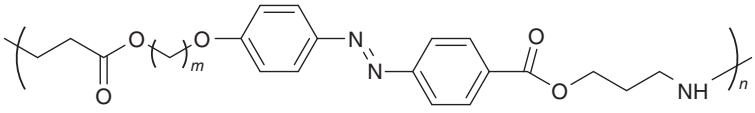

6

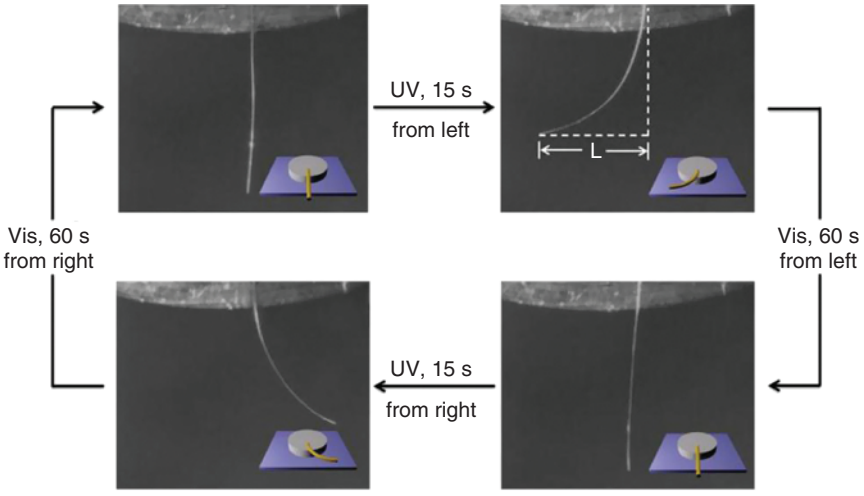

Figure 1.10 Photographs of the main-chain CLCP fiber that exhibit photoinduced bending and unbending behaviors upon irradiation with 365 nm UV light (150 mW cm^{-2}) and visible light ($\lambda > 430$ nm, 120 mW cm^{-2}) at 60 °C. The size of the fiber is 11 mm × 21 μm. (Fang *et al*. 2013 [39]. Reproduced with permission of American Chemical Society.)

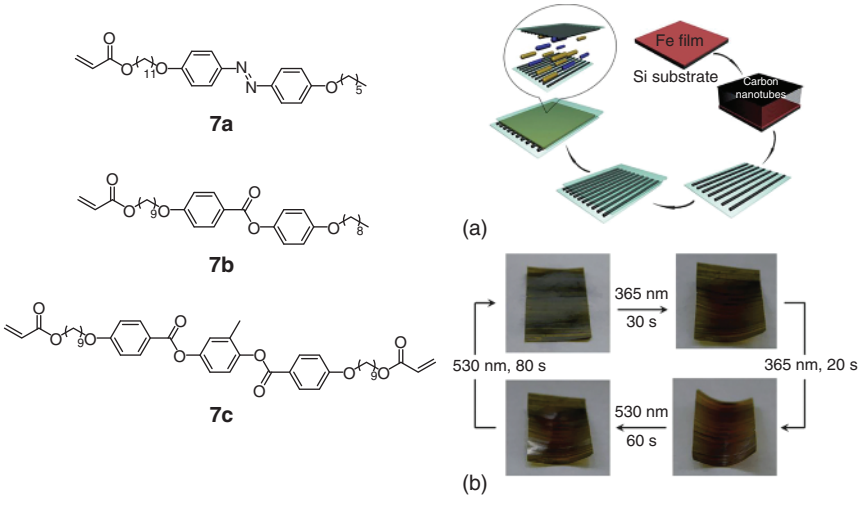

Figure 1.11 Chemical structure of two monomers **7a** and **7b**, and cross-linker **7c**. (a) Preparation of an oriented CLCP/CNT nanocomposite film. (b) Photographs of a CLCP/CNT composite film during one bending and unbending cycle after alternate irradiation by UV light at 365 nm (100 mW cm^{-2}) and visible light at 530 nm (35 mW cm^{-2}), respectively. (Wang *et al*. 2012 [40]. Reproduced with permission of Wiley.)

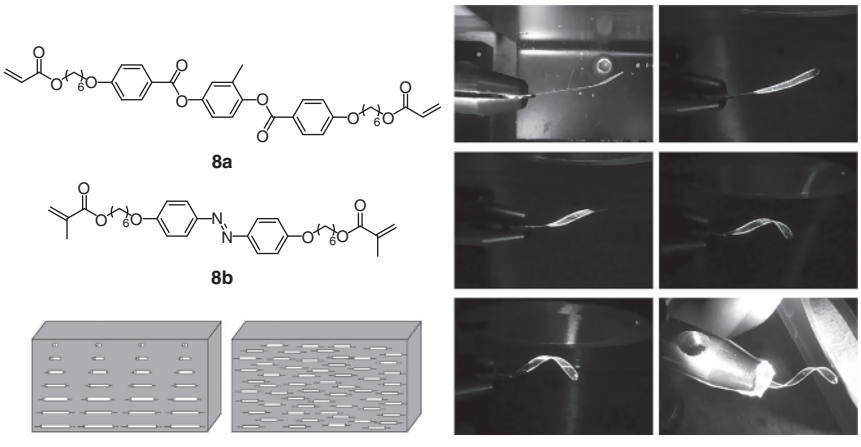

Figure 1.12 **8a** acts as the host mesogen, while the UV-active component is **8b**. (a) Schematic illustration of twisted and uniaxial arrangements. (b) Photoinduced coiling of a film in the twisted configuration. (Harris *et al*. 2005 [24]. Reproduced with permission of Royal Society of Chemistry.)

irradiation with UV light, the ribbons displayed winding, unwinding, and helix inversion, which results from the direction where the ribbons were cut. The cutting direction of the film is a parameter that determines not only the pitch and handedness of the helical shape that are formed, but also their photoinduced behavior (Figure 1.13).

1.4 Effect Factors of Photodeformation

In order to make clear the effect of the alignment of the azobenzene moieties on the photoinduced bending behavior of CLCP films, a variety of CLCP films with different alignment were examined. Homeotropically aligned films were prepared and showed a completely different bending direction compared with the homogenous CLCP films [43]. Upon exposure to UV light, these films underwent the bending away from the irradiation direction of the actinic light (Figure 1.14). Because the alignment direction of the azobenzene mesogens in the homeotropic films is perpendicular to the film surface, exposure to UV light causes an isotropic expansion contributing to the bending in a completely opposite direction. Furthermore, Ikeda *et al.* prepared CLCP films with a homogenous alignment on one surface and a homeotropic alignment on the opposite surface (hybrid alignment) and investigated their bending behavior [44]. Upon irradiation with UV light on the homogenous surface, the film bent toward the light source along the alignment direction, whereas the film bent away from the actinic light source when the homeotropic surface was irradiated. This illustrates that the bending direction is determined by the surface alignment treatment. Upon irradiation from both surfaces of the film, the bending speed was enhanced at the same time.

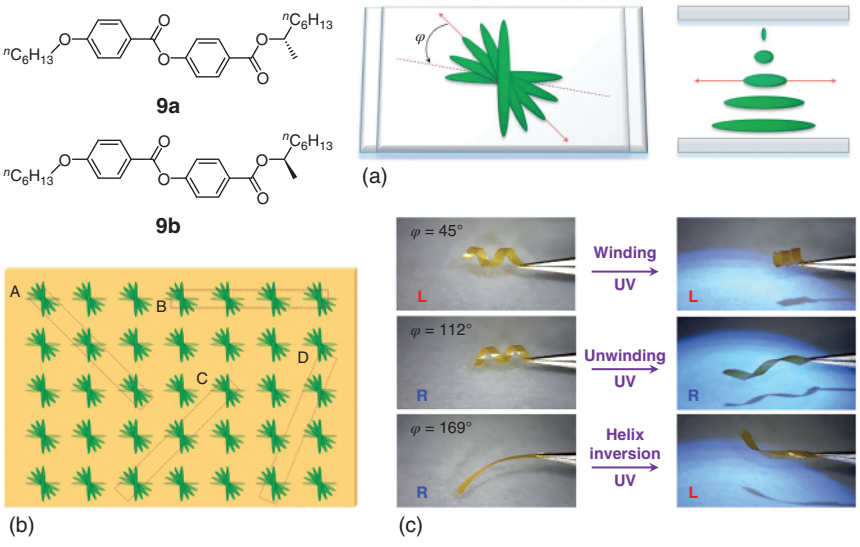

Figure 1.13 (a) Molecular organization in the twist cell (top view) and the angular offset φ, which characterizes the angle at which the ribbon is cut. The orientation of the molecules at mid-plane is shown with a double-headed arrow. The cutting direction, which is also the long axis of the ribbon, is represented by a dotted line. The elongated rods represent molecules (left) and the twist-nematic molecular orientation through the thickness of the film (side view) (right). (b) Schematic illustration showing the direction in which the ribbons are cut. (c) Spiral ribbons irradiated for 2 min with UV light ($\lambda = 365$ nm) display isochoric winding, unwinding, and helix inversion (φ was defined as the angle between the orientation of the molecules at mid-plane and the cutting direction; R: right-handed; L: left-handed). (Iamsaard *et al*. 2014 [42]. Reproduced with permission of Nature Publishing Group.)

The work described above suggests that the orientation states of the azobenzene mesogens have a strong effect on the bending behavior. Moreover, Ikeda *et al.* prepared a series of monodomain CLCP films with different cross-linking densities by copolymerization of Components **4a,b** and studied the effect of cross-linking density on photoinduced bending behavior of the oriented CLCP films [45]. The partially free-standing CLCP films were put on a glass substrate heated to the temperature higher than their glass transition temperature (T_g) by the hot stage. Upon exposure to UV light, the films showed the same bending behavior, but the maximum bending extent was different among the CLCP films with different cross-linking densities. The maximum bending extent increased with the increase of the cross-linking density. Because the increase of the cross-linking density leads to a higher order parameter of the films, the decrease in alignment order of azobenzene moieties causes a larger extent of bending of the film along this direction. In addition, the bending speeds, affected not only by the contraction at the film surface but also by the mobility of the polymer segments, were different for the films with different cross-linking densities.

Moreover, the effect of order degree of mesogens was investigated with the use of ferroelectric CLCP films. Compared with other liquid crystals, ferroelectric liquid crystals have two advantages: their high degree of order of mesogens, and

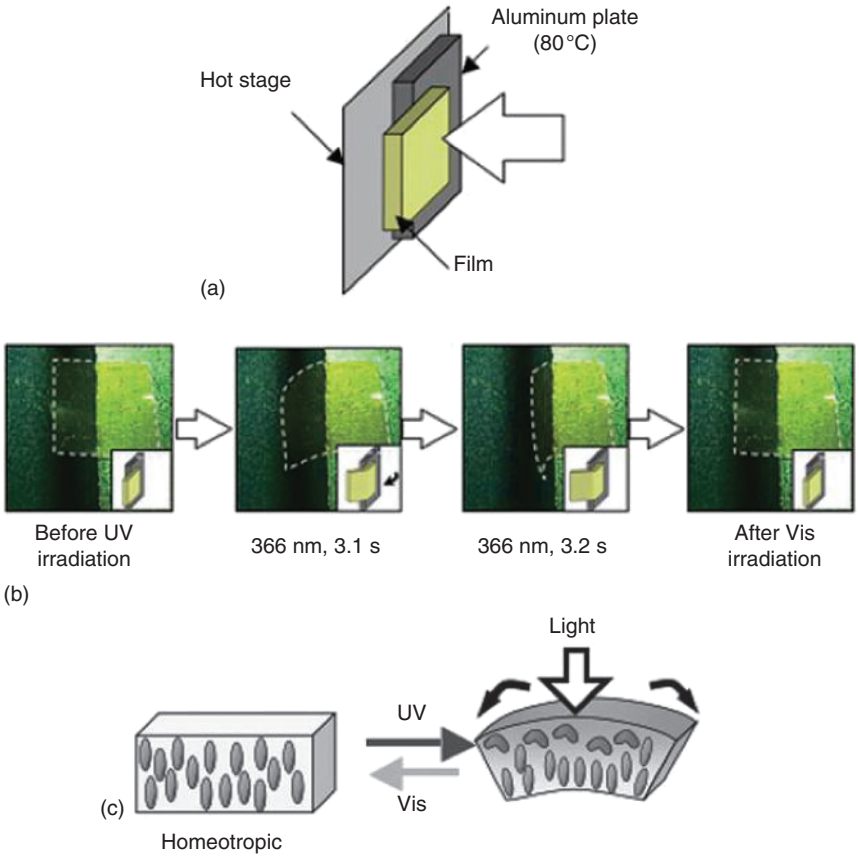

Figure 1.14 (a) Experimental setup and (b) photographs of the homeotropic film that exhibits photoinduced bending and unbending behavior. The white dash lines show the edges of the films, and the inset of each photograph is a schematic illustration of the film state. (c) Schematic illustration of the bending mechanism in the homeotropic film. (Iamsaard *et al*. 2014 [42]. Reproduced with permission of Nature Publishing Group.)

the fact that their molecular alignment can be controlled quickly by applying an electric field due to the presence of spontaneous polarization. Therefore, Ikeda *et al.* prepared ferroelectric CLCP films with a high LC order and a low T_g value by *in situ* photopolymerization of oriented LC Components **10a** and **10b** in the smectic C phase under an electric field (Figure 1.15) [46]. After irradiation with UV light, the films were found to bend toward the actinic light source with a tilt to the rubbing direction of the alignment layer, and the films reverted to their initial flat state upon exposure to visible light. The bending process was completed within 500 ms of irradiation by a laser beam, which is one order of magnitude faster than the bending of nematic CLCP films. Moreover, the mechanical force generated by photoirradiation reached about 220 kPa, similar to the contraction force of human muscles (around 330 kPa).

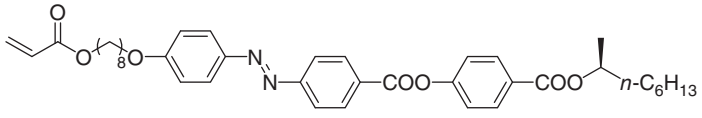

10a

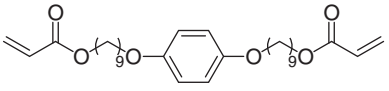

10b

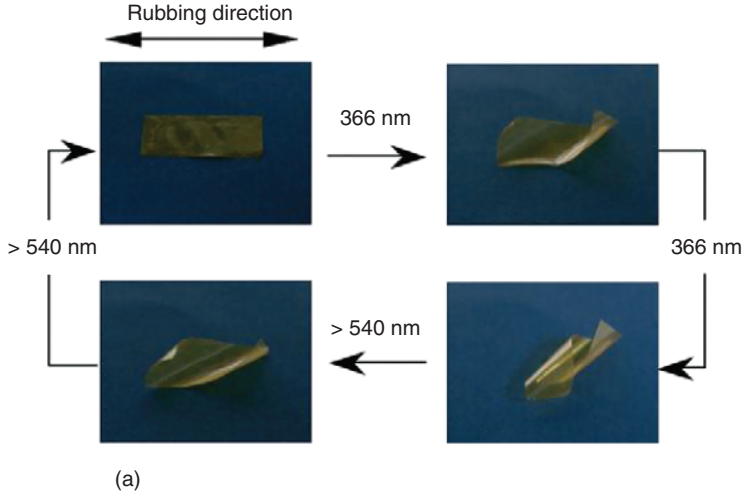

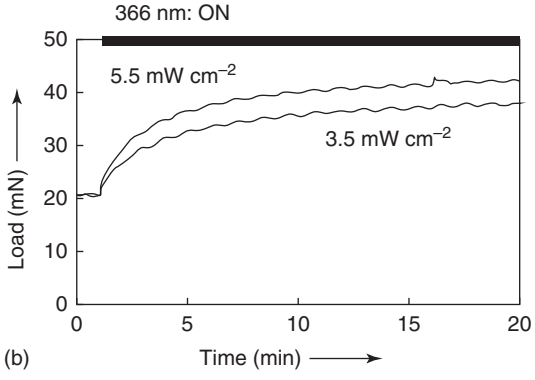

Figure 1.15 Photographs of the ferroelectric CLCP film that exhibits bending and unbending behavior upon alternative irradiation with UV and visible light at room temperature: the film bent toward the actinic light source along the alignment direction of mesogens in response to irradiation at $\lambda = 366$ nm, and were flattened again by irradiation with visible light at $\lambda > 540$ nm. (b) Change of the load on ferroelectric CLCP film when exposed to UV light at 366 nm with different intensities at 50 °C. The cross-section area of the film is 5 mm × 20 μm. An external force of 20 mN was loaded initially on the film to keep the length of the film unchanged. (Yu *et al*. 2006 [43]. Reproduced with permission of Wiley.)

The spacer length of the monomer and cross-linker is another key factor to bring about a different photoinduced deformation. As a connection of mesogens and main chains, spacer groups play an important role in determining the mesomorphic properties of polymer LCs [47]. It was also reported that the spacer length has much effect on the formation of LC phase [48]. In addition, the spacer affects the rigidity of polymer chains and therefore the T_g of the polymers. Yu and coworkers synthesized CLCP films with a long spacer by *in situ* photopolymerization of **11a** and **11b** [49]. Because of the relatively long spacer, the films

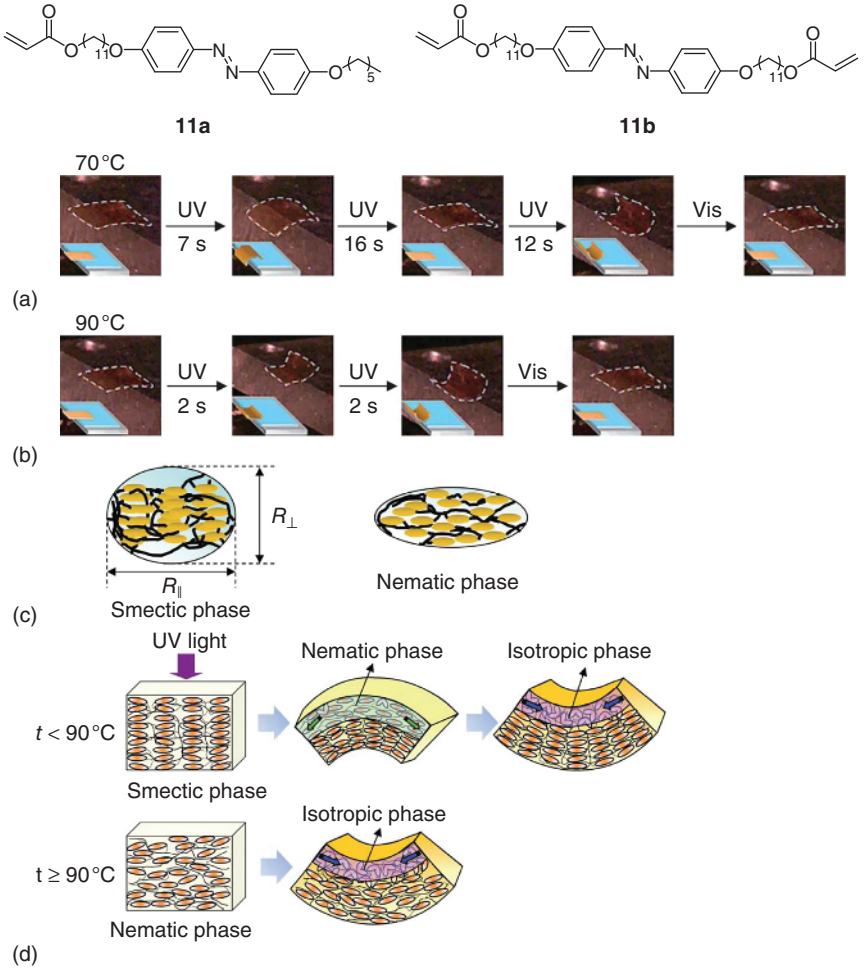

Figure 1.16 Photographs of CLCP film exhibiting different bending and unbending behavior at 70 °C (a) and 90 °C (b) upon irradiation of UV (366 nm, 18 mW cm^{-2}) and visible (>540 nm) light. The size of the film was 4 mm × 4 mm × 20 μm. A schematic illustration of (c) the mesogens alignment and the backbone conformation in the smectic and nematic phase and (d) a plausible mechanism of the different bending modes of the CLCP films at different temperatures. (Zhang *et al*. 2010 [49]. Reproduced with permission of Royal Society of Chemistry.)

exhibited a distinct photoinduced bending mode as shown in Figure 1.16. When the temperature was lower than 90 °C, the film first bent away from the light source along the alignment direction and then toward it upon the irradiation of UV light. However, when the temperature was raised above 90 °C, the film bent directly toward the light source. Since the isomerization rate of azobenzene chromophores in polymer matrix is slow, when some *cis*-azobenzene molecules appear upon the irradiation of UV light and break the high order of smectic phase, the film surface changes from smectic to nematic phase, showing a more prolate backbone conformation. Thus the surface region expands along the rubbing direction and the film bends away from the light source. As *cis*-azobenzene molecules begin to accumulate, the film surface subsequently changes from the nematic to the isotropic phase, leading to the contraction of the surface and the bending of the whole film toward the light source. When the temperature was raised above 90 °C, the film experienced a thermal phase transition from smectic to nematic. Upon exposure to UV light, the phase transition from nematic to isotropic resulted in the disordered backbone conformation and subsequently the contraction of the surface, thus the film tend directly toward the light source.

In addition to the alignment direction of the azobenzene moieties, the bending behavior of the films is also influenced by the location of the azobenzene moieties. Ikeda and coworkers prepared two azobenzene-containing CLCPs, both of which bear equal overall cross-linker concentrations and equal concentration of the azobenzene moieties but differ in their nature of binding of azobenzenes to the polymer network [50]. By changing the location of the photoactive azobenzene moieties from cross-links to side-chains, the bending direction is reversed under identical irradiation conditions. Therefore, they present a simple way to control the photoinduced bending direction of azobenzene-containing CLCPs.

1.5 Deformation Induced by Visible and NIR Light

To develop applications of light-driven organic actuators in possible biological systems, low energy light instead of UV light would be a more suitable stimulating source because low energy light penetrates deeper into tissues and causes less damage to biosamples. Moreover, as the stimulating source, UV light is not environment-friendly and does harm to our health, which limits the practical applications. Furthermore, sunlight is the origin of all the energy resources that can be endlessly supplied, and visible light is harmless and more abundant in sunlight. Thus, it would be useful to develop the CLCPs with photochromic molecules that undergo a photoinduced deformation in response to visible light, especially sunlight.

Yu *et al.* first reported visible light induced bending and unbending of azotolane-containing CLCPs, whose deformation even occurred upon exposure to sunlight [51, 52]. Compared with 366 nm absorption of usual azobenzene moieties, the maximum absorption of the azotolane groups shifts toward a long wavelength region at 385 nm, resulting in a decrease in the energy level difference between the π–π^* orbital of the tolane groups. Irradiated with short-wavelength

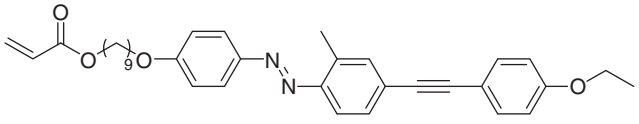

12a

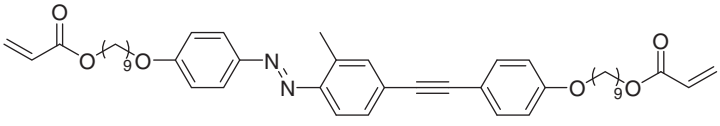

12b

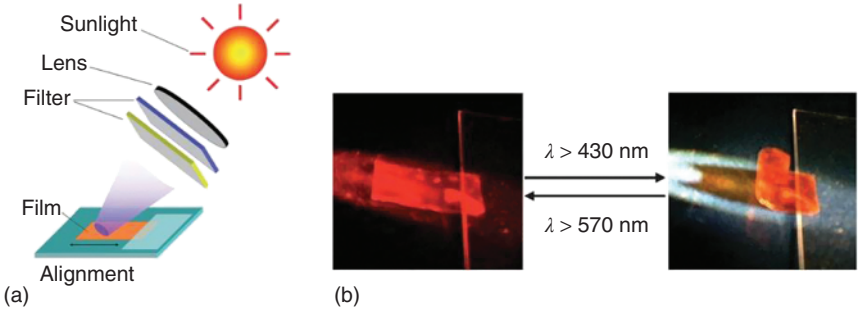

Figure 1.17 Chemical structures of the monomer **12a** and cross-linker **12b**. (a) Experimental setup. (b) Photoinduced bending and unbending behavior of azotolane CLCP film in sunlight through a lens and glass filters. The sunlight at >430 nm and at >570 nm was acquired by using different filters. (Yin *et al*. 2009 [52]. Reproduced with permission of Royal Society of Chemistry.)

visible light at 436 nm, the film bent toward the irradiation direction of the actinic light due to the trans–cis photoisomerization of azotolane and reverted to the initial state after irradiation with visible light at 577 nm. The azotolane CLCP film also underwent photoinduced bending and unbending behavior by means of manipulating the wavelength of sunlight through a lens and glass filters as shown in Figure 1.17. This kind of sunlight-responsive film is of great importance in the development and utilization of solar energy because it converts solar energy into mechanical energy directly.

Furthermore, Yu *et al.* gave the first example to incorporate upconversion nanophosphors (UCNPs) $NaYF_4$:Yb,Tm into the azotolane-containing CLCP film and succeed in generating fast bending of the resulting composite film upon irradiation with continuous-wave (CW) NIR light at 980 nm (Figure 1.18a) [53]. Here, upconversion luminescence (UCL) of the nanophosphors not only induces trans–cis photoisomerization of the azo groups but also leads to alignment change of the mesogens. Under excitation with a CW 980 nm laser, the as-prepared UCNPs shows blue emission and the main UCL emission peaks at 450 and 475 nm, as shown in Figure 1.18b, overlap the absorption band of the azotolane CLCP film (between 320 and 550 nm) perfectly; thus, the UCL light emitted by UCNPs triggers the trans–cis photoisomerization of the azotolane

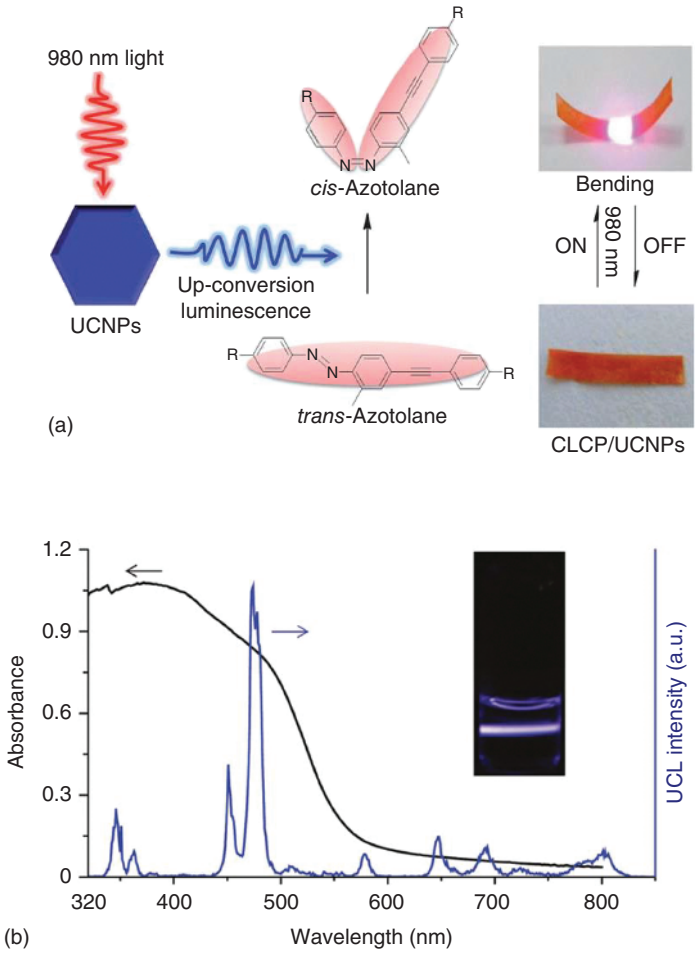

Figure 1.18 Schematic illustration of the mechanism of CW NIR-light-induced deformation of the azotolane CLCP/UCNP composite film, and photographic frames of the composite film bending in response to the NIR light at CW 980 nm and being flattened after removing the light source. (b) UCL emission spectrum (blue line) of a colloidal $CHCl_3$ solution of UCNPs (1 mg ml^{-1}) excited with a 980 nm CW laser (power = 600 mW, power density = 15 W cm^{-2}) and the UV–vis absorption spectrum (black line) of azotolane CLCP film. The inset shows a photograph of UCL from the UCNPs in $CHCl_3$. (Wu *et al*. 2011 [53]. Reproduced with permission of American Chemical Society.)

moieties. This kind of novel photodeformable CLCP system is promising for biological applications, since NIR light penetrates deeper into tissues and creates less damage to biosamples.

Lately, Yu *et al.* achieved a red-light controllable composite film driven by low-power excited UCL based on triplet–triplet annihilation (TTA) [54]. This TTA-based UCL process shows several advantages over the lanthanide upconversion techniques, such as higher quantum efficiency, large absorption efficiency, and low excitation power density. When PtTPBP (**13a**) and BDPPA

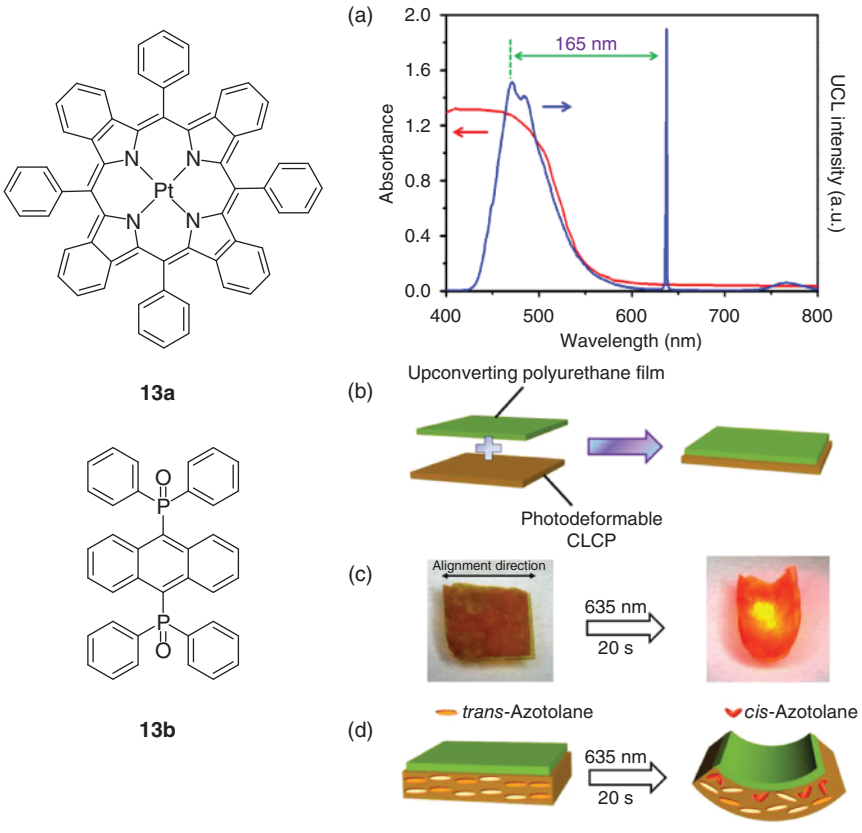

Figure 1.19 Chemical structures of the sensitizer PtTPBP (**13a**) and the annihilator BDPPA (**13b**). (a) UCL emission spectrum (blue line) of toluene solution of PtTPBP&BDPPA (λ_{ex} = 635 nm, power density = 200 mW cm^{-2}) and the UV–vis absorption spectrum (red line) of the azotolane CLCP film. (b) Schematic illustration of the preparation of the assembly film composed of azotolane CLCP film and PtTPBP&BDPPA-containing polyurethane film. (c) Photographs of the as-prepared assembly film bending toward the light source along the alignment direction of the mesogens in response to the 635 nm laser with the power density of 200 mW cm^{-2} (thickness of each layer in the assembly film: 15 μm of upconverting film and 27 μm of CLCP film). (d) Schematic illustration demonstrating plausible mechanism for the photoinduced deformation of the as-prepared assembly film. (Jiang *et al*. 2013 [54]. Reproduced with permission of American Chemical Society.)

(**13b**) were incorporated into a soft polyurethane film and then assembled with an azotolane-containing CLCP film, a soft material system was achieved (Figure 1.19). Upon excitation of 635 nm laser, the PtTPBP&BDPPA-containing polyurethane film acts as an antenna to trap the 635 nm light and upconvert it into the blue (triplet–triplet annihilation-upconversion luminescence) TTA-UCL emission; then the TTA-UCL is absorbed by the azotolane moieties in the CLCP film via the emission–reabsorption process, which induces the trans–cis photoisomerization of the azotolane moieties and the subsequent alignment change of the mesogens, thus contributing to the photoinduced bending of the azotolane CLCP film toward the light source. Moreover, to our

most interest, the assembly film still bent toward the light source even though a piece of pork with the thickness of 3 mm was put between the light source and assembly film, which demonstrates potential biological applications using this novel red-light-controllable soft actuator. This work not only provides a novel photomanipulated soft actuation material system based on the TTA-UCL technology but also introduces a new technological application of the TTA-based upconversion system in photonic devices.

1.6 Soft Actuators Based on CLCPs

An actuator is an energy transducer that can convert input energies of a variety of forms into mechanical quantities such as displacement, strain, velocity, and stress [17]. Artificial muscle-like actuators are receiving great interest for use as novel devices, because they are ideal for the realization of biomimetic movements by changing their shapes and dimensions. Since large deformation can be generated in CLCPs with the help of photochemical reaction of chromophores, light-driven soft CLCPs thus play an important role in realizing soft actuators, which can convert light energy into mechanical work directly by using a contactless laser beam.

1.6.1 Macro-scaled Actuators

Ikeda *et al.* reported the first light-driven plastic motor with laminated films composed of a CLCP film and a polyethylene sheet [55]. A continuous plastic belt of the CLCP laminated film was prepared by connecting both ends of the film, and then placing the belt on a homemade pulley system as illustrated in Figure 1.20a. By irradiating the belt with UV light from top right and visible light from top left simultaneously, a rotation of the belt was induced to drive the two pulleys in a counterclockwise direction at room temperature, as shown in Figure 1.20b. Furthermore, they demonstrated a unidirectional motion, an inchworm walk, of the CLCP laminated film with asymmetric end shapes [56]. The film moved forward upon alternate irradiation with UV and visible light (Figure 1.20c). Additionally, they also showed such creative three-dimensional movements as a flexible robotic arm motion assembled with the CLCP laminated film.

van Oosten *et al.* succeeded in producing artificial cilia through inkjet printing [57]. The deposition with an inkjet printer allows different LC materials to be arranged perpendicular to the substrate at the bottom and parallel to the substrate at the top of the film. The cilia consisted of two different azobenzene chromophores: one sensitive to UV light, the other to visible light. Thus, asymmetric motion can be induced only by varying the light intensity over the actuator surface (Figure 1.21).

Instead of covalently linking the azobenzene moiety to the elastomer, Palffy-Muhoray and coworkers created CLCP with an azo-dye dispersed in it [58]. When floating on water, the CLCP was found to swim into the darker regions, namely, away from the laser beam as a result of exchanging momentum between water and the sample upon its bending motion.

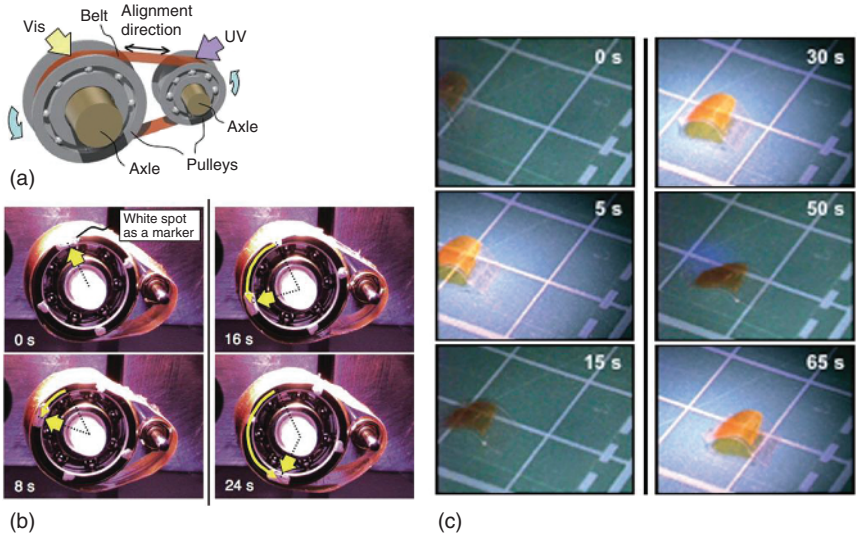

Figure 1.20 (a) Schematic illustration of a light-driven plastic motor system used, showing the relationship between light irradiation positions and a rotation direction. (b) Photographs showing time profiles of the rotation of the light-driven plastic motor with the CLCP-laminated film induced by simultaneous irradiation with UV and visible light at room temperature. (c) Series of photographs showing time profiles of the photoinduced inchworm walk of the CLCP laminated film by alternative irradiation with UV (366 nm, 240 mW cm^{-2}) and visible light (>540 nm, 120 mW cm^{-2}) at room temperature. The film moved on the plate with 1 cm × 1 cm grid. Size of the film: 11 mm × 5 mm; the CLCP laminated part: 6 mm × 4 mm. Thickness of the layers of the film: PE, 50 μm; CLCP, 18 μm. (Yamada *et al*. 2008 [55]. Reproduced with permission of Wiley.)(Yamada *et al*. 2008 [55]. Reproduced with permission of Royal Society of Chemistry.)

Yu *et al.* prepared a visible-light-driven fully plastic microrobot [59]. The microrobot was made of CLCP and PE bilayer films and consisted of several parts, including a hand, a wrist, and an arm (Figure 1.22). Without the aid of any gears, bearings, or contact-based driving systems, the microrobot was manipulated to pick, lift, move, and place milligram-scale objects by irradiating different parts of the microrobot with visible light.

Zhu *et al.* designed a model of photoactivated micropump, mainly including photodeformable material, pump membrane, pump chamber, and pipes (Figure 1.23) [60]. Water is chosen as the pump medium. The flow rate of the water varied in a stroke of the pump membrane, which means, the bending speed of the laminated film decreased in this process. The smaller pressure would lead to a higher flow rate and a larger volume pumped in a stroke. In a further study, they utilized the bending of CLCP films to act as a valve membrane [61].

1.6.2 Micro-scaled Actuators

Yu *et al.* designed and fabricated a light-regulated adhesion switch on a micro-arrayed azobenzene CLCP superhydrophobic surface, by which water droplets could be rapidly, precisely, locally, and through no contact, controlled [62]. It is well known that surface chemical composition as well as a suitable

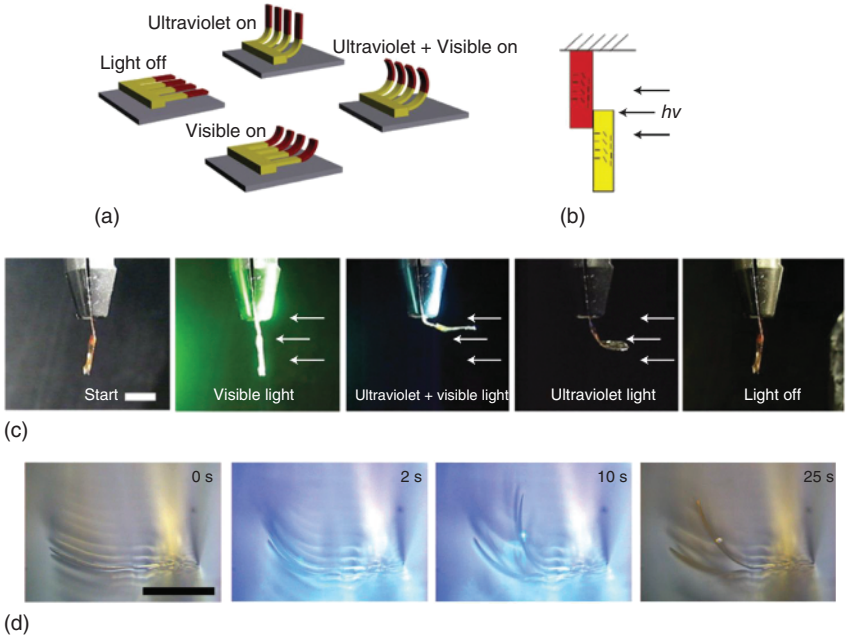

Figure 1.21 (a) Artificial, light-driven cilia produce an asymmetric motion controlled by the spectral composition of the light. (b) Schematic representation of the macroscopic setup, showing the orientation of the molecules. (c) Steady-state responses of a 10-μm-thick, 3-mm-wide, and 10-mm-long modular liquid-crystal network actuator to different colors of light (scale bar 5 mm). (d) Side view of the actuation of polymer cilia with ultraviolet light (1 W cm^{-2}) in water. (van Oosten *et al*. [57].)

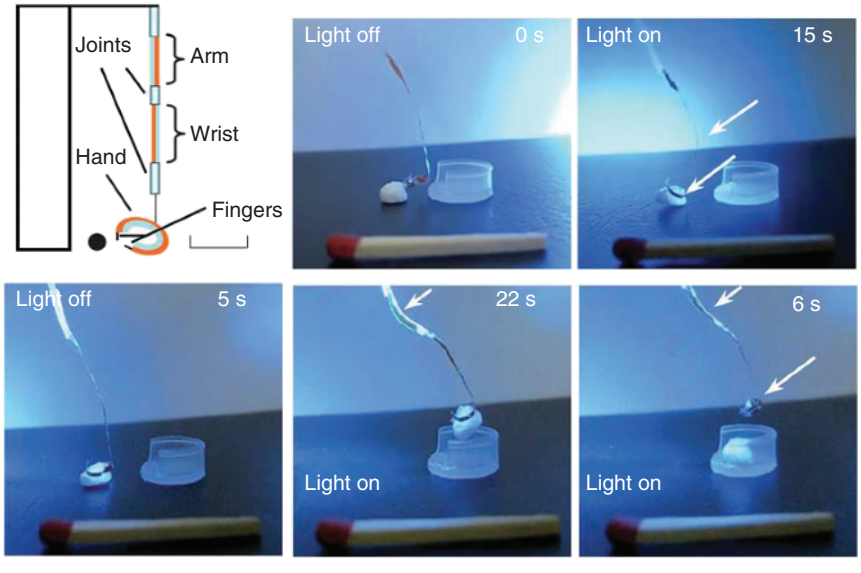

Figure 1.22 Schematic illustration of the microrobot and photographs showing microrobot picking, lifting, moving, and placing the object to a nearby container by turning on and off the light (470 nm, 30 mW cm^{-2}). The thickness of both PE and films was 20 μm. They were connected with each other by the adhesive. White arrows denote the parts irradiated with visible light. (Cheng *et al*. 2010 [59]. Reproduced with permission of Royal Society of Chemistry.)

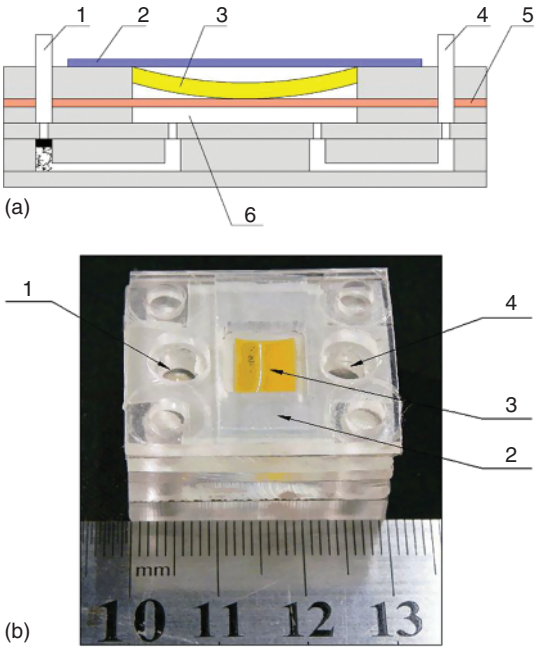

Figure 1.23 (a) The section of assembled prototype. (b) Photo of experimental prototype (1, inlet; 2, press plate; 3, photodeformable material; 4, outlet; 5, pump membrane; 6, pump chamber). (Jiang *et al*. 2013 [54]. Reproduced with permission of Royal Society of Chemistry.)

micro/nanoscale rough surface cooperatively creates superhydrophobicity. Polydimethylsiloxane-soft-template-based secondary replication was utilized to introduce uniform and quantitatively controllable surface roughness to the azobenzene CLCP film. After UV light irradiation, the azobenzene mesogens at the surface of the film transferred to a cis state and the water adhesion increased because of the growth of surface polarity, since in the excited cis-configuration, the dipole moment leads to an increase of local polarity of polymer chain. Subsequently, after the visible light irradiation, the azobenzene mesogens at the surface returned to the trans state and the surface reverted to lower adhesive superhydrophobic state (Figure 1.24). Such a quick and reversible switch of superhydrophobic adhesion was retained well after many cycles by the alternate irradiation of UV and visible light. Unlike contact angle (CA) switchable surfaces systems, our work put emphasis on the switching of sliding angle (SA) on the same surface, while the static CAs before and after switching were all in the superhydrophobic range. Therefore, the "rolling" and "pinning" of water droplets was achieved, giving rising to promising applications in microfluids. It is the first time that the photoresponsive CLCP materials were used to prepare superhydrophobic adhesion switchable surfaces, which is of great importance for no-loss microdroplet transfer.

Most recently, Yu *et al.* successfully fabricated CLCP films with different surface topographies, submicropillar, and submicrocone arrays, through colloidal lithography technique by modulating different types of etching masks [63]. The prepared submicropillar arrays were uniform with an average pillar diameter of 250 nm and the cone bottom diameter of the submicrocone arrays was about 400 nm, which are much smaller than previously reported CLCP micropillars.

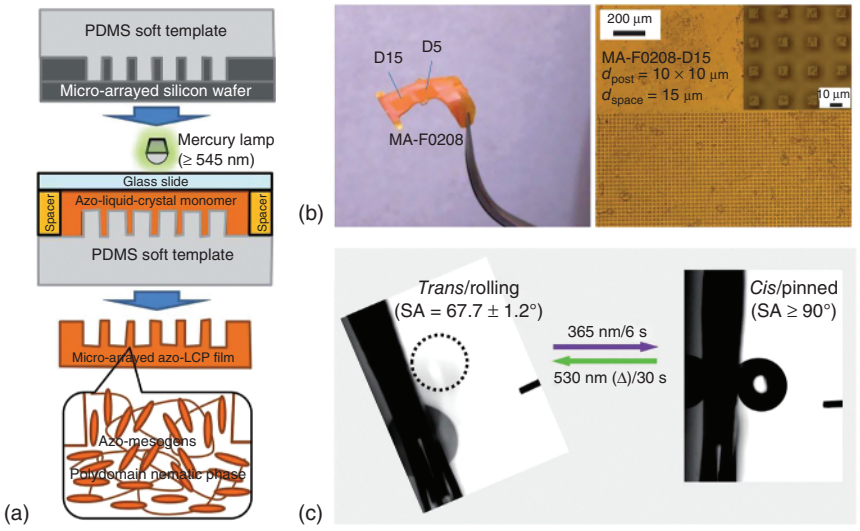

Figure 1.24 (a) Schematic illustration of the PDMS-soft-template-based secondary replication process. (b) Optical photo of microarrayed CLCP film with two patterned areas named as D15 and D5. Large-area optical microscopic image and local amplified image (inset). The patterns of D15 and D5 are all square-arrayed square posts with the post width of 10 mm. The spacings between two nearest posts for D15 and D5 are 15 and 5 mm, respectively. (c) Light-controlled quick and reversible switching of superhydrophobic adhesion between rolling and pinning on microarray CLCP with a 2 μl water droplet. (Li *et al*. 2012 [62]. Reproduced with permission of Royal Society of Chemistry.)

More interestingly, these two species of films with the same chemical structure represented completely different wetting behavior of water adhesion and mimicked the rose petal and lotus leaf, respectively. Both the submicropillar arrayed film and the submicrocone arrayed film exhibited superhydrophobicity with a water contact angle (CA) value of $144.0 \pm 1.7°$ and $156.4 \pm 1.2°$, respectively. Meanwhile, the former demonstrated a very high sliding angle (SA) greater than 90°, and thus, the water droplet was pinned on the surface as in a rose petal. On the contrary, the SA of the submicrocone arrayed CLCP film consisting of micro- and nanostructure was only $3.1 \pm 2.0°$, which is as low as that of the lotus leaf. Compared to replica molding technique and inkjet printing technology that are used to fabricate microstructured CLCPs, colloidal lithography technique is time-saving and can be modulated throughout etching procedure, which finely regulates the structural parameters such as shapes and dimensions. Our work provides a new way to fabricate the CLCPs in the size of a nanoscale.

Yu *et al.* fabricated a photoresponsive 2D microarray with a period of about 1 μm using CLCP containing azobenzene groups by using the replica molding technique [64]. The CLCP microarray showed switchable behavior on the reflection spectra by alternate irradiation of UV and visible light, accompanied by the deformation of the CLCP pillars. Because the trans–cis photoisomerization results in the alignment change of LC molecules especially in the side surface region of pillars, the pillars contract along the long axis while they

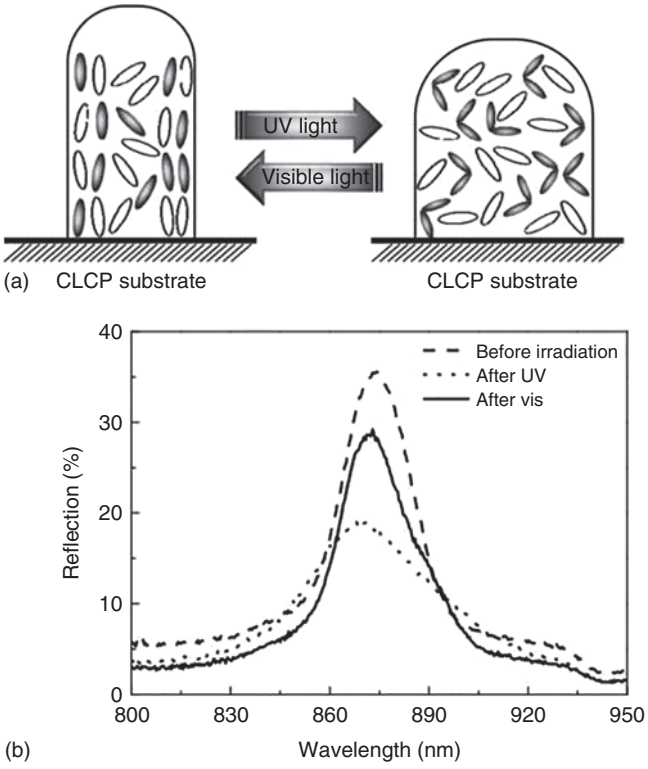

Figure 1.25 (a) Schematic illustration showing the change in the geometry of the pillars of the azobenzene CLCP microarray. (b) Reflection spectra of the azobenzene CLCP microarray under the UV light irradiation (365 nm, 20 mW cm^{-2}, 15 min) and the following visible light irradiation (530 nm, 20 mW cm^{-2}, 5 min) with the angle of incidence of 60°.

undergo expansion along the short axis, leading to the increase in the diameter of the pillars and variation in the reflection spectra of the CLCP microarray (Figure 1.25). This is the first time the CLCP was used to fabricate the microarray with a period of about 1 μm and manipulate switchable behavior on the reflection spectra of the LC polymer microarray by light.

Furthermore, Yu *et al.* prepared novel photo and thermal dual-responsive inverse opal films based on CLCP [65]. The inverse opal film showed switchable behavior on the reflection spectra by alternate irradiation of UV and visible light or temperature, owing to the change in the order of the holes. This change in the periodic structure is ascribed to the contraction of CLCP induced by the photochemical reactions of the azobenzene moieties or the thermal-induced phase transition. The optical properties drastically decreased by thermal or photoinduced phase transitions of the CLCP (Figure 1.26). It is the first time that azobenzene-containing CLCPs have been used to prepare inverse opal film and achieve repeatable switching behavior on the reflection spectra of film by using light, which can be manipulated conveniently and controlled *in situ*. The reflectivity changed to a greater extent compared to the 2D CLCP photonic crystals.

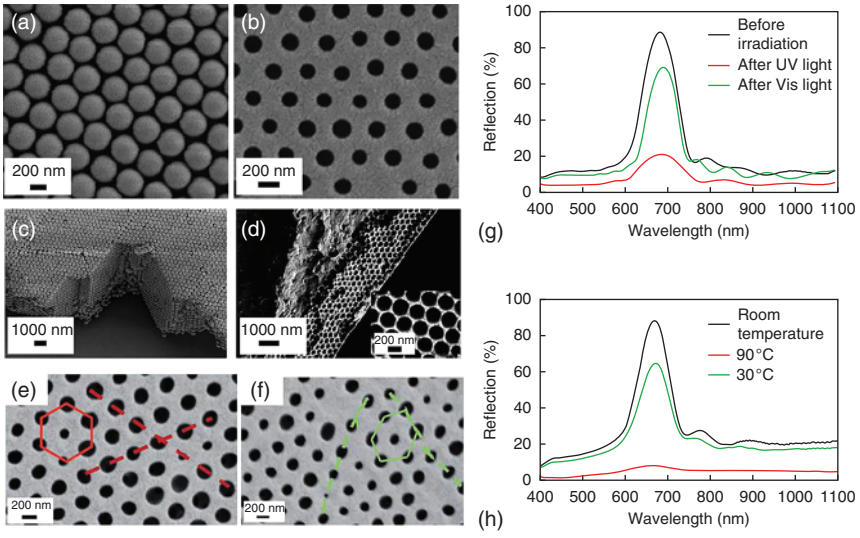

Figure 1.26 SEM surface images of (a) the SiO_2 opal film and (b) the CLCP inverse opal film, and SEM cross-section images of (c) the SiO_2 opal film and (d) the CLCP inverse opal film. The inset is the locally amplified image. Thickness of the inverse opal film is about 17 mm. SEM images of the inverse opal film (e) before and (f) after UV light irradiation. The red regular hexagon and straight lines represent the arrangement of the holes before UV light irradiation; the green hexagon and lines represent the arrangement of the holes after irradiation with UV light. After UV light irradiation, the shape of the hexagon becomes irregular, and the straight lines have become curves. (g) Reflection spectra of the azobenzene CLCP inverse opal film under UV light irradiation (365 nm, 50 mW cm^{-2}, 5 min) and subsequent visible light irradiation (530 nm, 20 mW cm^{-2}, 15 min). (h) Reflection spectra of the inverse opal film as a function of temperature. (Zhao *et al*. 2014 [65]. Reproduced with permission of Royal Society of Chemistry.)

Wiersma *et al.* used direct laser writing system to pattern the complex 3D structures with sub-micrometer resolution [66, 67]. Microrobots were fabricated with the CLCPs acting as the main body of walkers [68]. The light-induced maximum stress of these systems was measured to be 260 ± 2 kPa, which was comparable to natural muscles (10–200 kPa). The legs of walkers had a conical shape, which was chosen to reduce the surface contact area, while 45° tilt of the leg created asymmetry adhesion necessary for walking (Figure 1.27a,b). The artificial creature automatically performed various locomotive activities that were highly dependent on the interactions with the environment. The microscopic walker finished random or directional walking, rotating, or jumping when placed on surfaces with different treating methods (Figure 1.27c).

1.7 Summary

The incorporation of photochromic moieties makes it possible for the CLCPs to be photoresponsive and the resultant actuators to be photo-driven. Upon irradiation of UV light, trans–cis photoisomerization of the azobenzene moieties

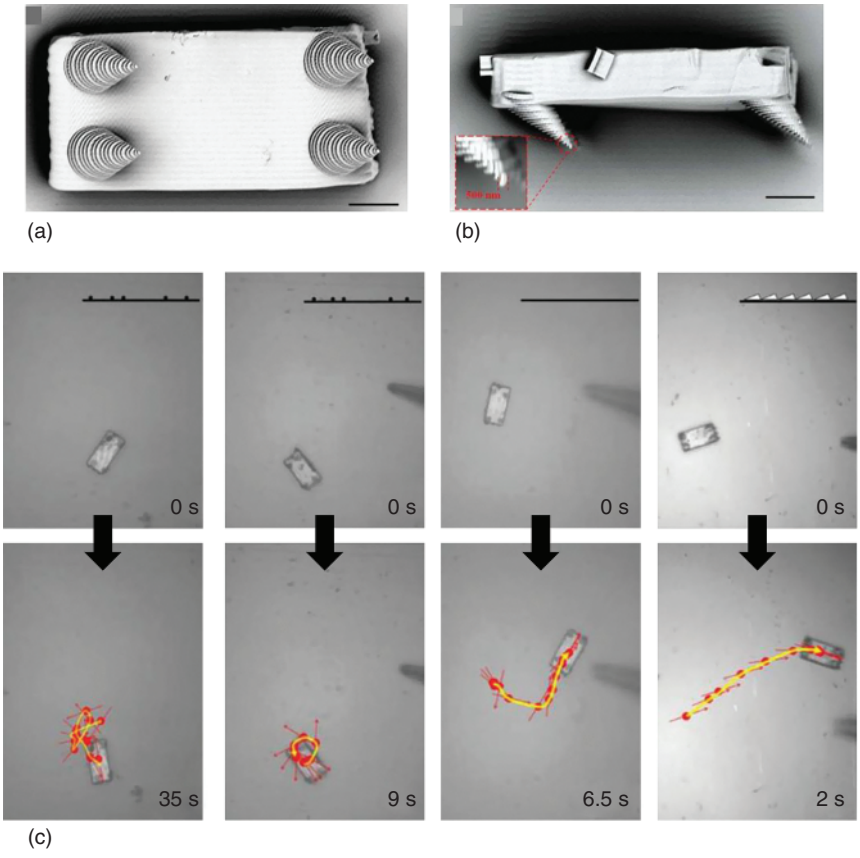

Figure 1.27 (a) SEM image of a microwalker lying upside down. Scale bar: 10 μm. (b) Side view of the microwalker with 500 nm leg tip shown in the inset. Scale bar: 10 μm. (c) Top row shows the initial state of microwalkers on different surfaces. Bottom row shows the microwalker randomly walking on the polyimide coated glass surface, rotating with one leg stuck onto the polyimide coated surface, walking with self-reorientation on the clean glass surface, walking in the direction determined by the grating groove pattern (vertical). Insets of the top row show the schematics of the surface. (Zeng *et al*. 2015 [68]. Reproduced with permission of Wiley.)

in the CLCPs is triggered, which leads to the change in the alignment of the mesogens; subsequently, the significant macroscopic photodeformation of the whole materials in the form of contraction, bending, and twisting was induced due to the cooperative motion of mesogens and polymer segments. In order to make the CLCPs responsive to longer wavelength light based on the considerations of safety, power consumption, and cost, the long conjugated group has been combined to the photochromic mesogens and the upconversion materials have been incorporated into the CLCP systems, which contribute to the deformation triggered by blue light, red light, and even NIR light. Furthermore, the photodeformable CLCPs have been developed as various soft actuators such as plastic motors, inchworm-like walkers, and flexible microrobots.

Due to their photocontrollable properties without any aid of other motors, gears, and wires, it is very convenient and attractive to reduce the size of the photo-driven CLCP actuators for their potential application in micro- and even nanoscales. So far, the microarrayed CLCP films, the inverse opal CLCP films, the cilia-like microactuators, and the microwalkers have been developed based on the replica molding, inject printing technique, and laser writing systems. In addition, the size of the photo-driven actuators has been successfully diminished to the nanoscale by colloidal lithography techniques. These make it advantageous to use photo-driven CLCP actuators in a wide range of potential application fields such as microfluid systems, micro-opto-mechanical systems (MOMSs) and optical devices.

However, further efforts are still needed to make them of value in real life applications. For instance, the improvement of the energy conversion efficiency, fatigue resistance and strength, and the continuous production of CLCPs remain challenges for researchers. In addition, there is an urgent need to integrate the CLCPs into functional and sophisticated devices with other materials because of the difficulty of the photo-responsive CLCPs to serve as the whole smart devices in real applications.

References

1 Bar-Cohen, Y. and Zhang, Q.M. (2008) Electroactive polymer actuators and sensors. *MRS Bull.*, **33**, 173–181.

2 Habault, D., Zhang, H.J., and Zhao, Y. (2013) Light-triggered self-healing and shape-memory polymers. *Chem. Soc. Rev.*, **42**, 7244–7256.

3 Wei, J. and Yu, Y.L. (2012) Photodeformable polymer gels and crosslinked liquid-crystalline polymers. *Soft Matter*, **8**, 8050–8059.

4 Xie, P. and Zhang, R.B. (2005) Liquid crystal elastomers, networks and gels: advanced smart materials. *J. Mater. Chem.*, **15**, 2529–2550.

5 Yu, Y.L. and Ikeda, T. (2006) Soft actuators based on liquid-crystalline elastomers. *Angew. Chem. Int. Ed.*, **45**, 5416–5418.

6 Chaterji, S., Kwon, I.K., and Park, K. (2007) Smart polymeric gels: redefining the limits of biomedical devices. *Prog. Polym. Sci.*, **32**, 1083–1122.

7 Leng, J.S., Lan, X., Liu, Y.J., and Du, S.Y. (2011) Shape-memory polymers and their composites: Stimulus methods and applications. *Prog. Mater Sci.*, **56**, 1077–1135.

8 Lendlein, A. and Kelch, S. (2002) Shape-memory polymers. *Angew. Chem. Int. Ed.*, **41**, 2035–2057.

9 Ilievski, F., Mazzeo, A.D., Shepherd, R.E., Chen, X., and Whitesides, G.M. (2011) Soft robotics for chemists. *Angew. Chem. Int. Ed.*, **50**, 1890–1895.

10 Harris, K.D., Bastiaansen, C.W.M., Lub, J., and Broer, D.J. (2005) Self-assembled polymer films for controlled agent-driven motion. *Nano Lett.*, **5**, 1857–1860.

11 Leng, J.S., Huang, W.M., Lan, X., Liu, Y.J., and Du, S.Y. (2008) Significantly reducing electrical resistivity by forming conductive Ni chains in a

polyurethane shape-memory polymer/carbon-black composite. *Appl. Phys. Lett.*, **92**, 204108.

12 Moschou, E.A., Madou, M.J., Bachas, L.G., and Daunert, S. (2006) Voltage-switchable artificial muscles actuating at near neutral pH. *Sens. Actuators, B*, **115**, 379–383.

13 Mohr, R., Kratz, K., Weigel, T., Lucka-Gabor, M., Moneke, M., and Lendlein, A. (2006) Initiation of shape-memory effect by inductive heating of magnetic nanoparticles in thermoplastic polymers. *Proc. Natl. Acad. Sci. U.S.A.*, **103**, 3540–3545.

14 Finkelmann, H. (1987) Liquid-crystalline polymers. *Angew. Chem. Int. Ed. Engl.*, **26**, 816–824.

15 Fleischmann, E.K. and Zentel, R. (2013) Liquid-crystalline ordering as a concept in materials science: from semiconductors to stimuli-responsive devices. *Angew. Chem. Int. Ed.*, **52**, 8810–8827.

16 White, T.J. and Broer, D.J. (2015) Programmable and adaptive mechanics with liquid crystal polymer networks and elastomers. *Nat. Mater.*, **14**, 1087–1098.

17 Ikeda, T., Mamiya, J., and Yu, Y.L. (2007) Photomechanics of liquid-crystalline elastomers and other polymers. *Angew. Chem. Int. Ed.*, **46**, 506–528.

18 Ube, T. and Ikeda, T. (2014) Photomobile polymer materials with crosslinked liquid-crystalline structures: molecular design, fabrication, and functions. *Angew. Chem. Int. Ed.*, **53**, 10290–10299.

19 Degennes, P.G. (1975) One type of nematic polymers. *Cr. Acad. Sci. B. Phys.*, **281**, 101–103.

20 Ohm, C., Brehmer, M., and Zentel, R. (2010) Liquid crystalline elastomers as actuators and sensors. *Adv. Mater.*, **22**, 3366–3387.

21 Finkelmann, H., Nishikawa, E., Pereira, G.G., and Warner, M. (2001) A new opto-mechanical effect in solids. *Phys. Rev. Lett.*, **87**, 015501 1–4.

22 Hiraoka, K., Sagano, W., Nose, T., and Finkelmann, H. (2005) Biaxial shape memory effect exhibited by monodomain chiral smectic C elastomers. *Macromolecules*, **38**, 7352–7357.

23 Li, M.H., Keller, P., Yang, J.Y., and Albouy, P.A. (2004) An artificial muscle with lamellar structure based on a nematic triblock copolymer. *Adv. Mater.*, **16**, 1922–1925.

24 Mol, G.N., Harris, K.D., Bastiaansen, C.W.M., and Broer, D.J. (2005) Thermo-mechanical responses of liquid-crystal networks with a splayed molecular organization. *Adv. Funct. Mater.*, **15**, 1155–1159.

25 Fleischmann, E.-K., Romina Forst, F., Katrin, K., Nadia, K., and Rudolf, Z. (2013) *J. Mater. Chem. C*, **1**, 5885–5891.

26 Tazuke, S., Kurihara, S., and Ikeda, T. (1987) Amplified image recording in liquid-crystal media by means of photochemically triggered phase-transition. *Chem. Lett.*, **16**, 911–914.

27 Ikeda, T. (2003) Photomodulation of liquid crystal orientations for photonic applications. *J. Mater. Chem.*, **13**, 2037–2057.

28 Ikeda, T., Horiuchi, S., Karanjit, D.B., Kurihara, S., and Tazuke, S. (1988) Photochemical image storage in polymer liquid-crystals. *Chem. Lett.*, **17**, 1679–1682.

29 Ikeda, T., Horiuchi, S., Karanjit, D.B., Kurihara, S., and Tazuke, S. (1990) Photochemically induced isothermal phase-transition in polymer liquid-crystals with mesogenic phenyl benzoate side-chains. 1. Calorimetric studies and order parameters. *Macromolecules*, **23**, 36–42.

30 Ikeda, T., Horiuchi, S., Karanjit, D.B., Kurihara, S., and Tazuke, S. (1990) Photochemically induced isothermal phase-transition in polymer liquid-crystals with mesogenic phenyl benzoate side-chains. 2. Photochemically induced isothermal phase-transition behaviors. *Macromolecules*, **23**, 42–48.

31 Cviklinski, J., Tajbakhsh, A.R., and Terentjev, E.M. (2002) UV isomerisation in nematic elastomers as a route to photo-mechanical transducer. *Eur. Phys. J. E*, **9**, 427–434.

32 Hogan, P.M., Tajbakhsh, A.R., and Terentjev, E.M. (2002) UV manipulation of order and macroscopic shape in nematic elastomers. *Phys. Rev. E*, **65**, 041720.

33 Li, M.H., Keller, P., Li, B., Wang, X.G., and Brunet, M. (2003) Light-driven side-on nematic elastomer actuators. *Adv. Mater.*, **15**, 569–572.

34 Ikeda, T., Nakano, M., Yu, Y.L., Tsutsumi, O., and Kanazawa, A. (2003) Anisotropic bending and unbending behavior of azobenzene liquid-crystalline gels by light exposure. *Adv. Mater.*, **15**, 201–205.

35 Yu, Y.L., Nakano, M., and Ikeda, T. (2003) Directed bending of a polymer film by light – miniaturizing a simple photomechanical system could expand its range of applications. *Nature*, **425**, 145.

36 Mamiya, J.I., Yoshitake, A., Kondo, M., Yu, Y., and Ikeda, T. (2008) Is chemical crosslinking necessary for the photoinduced bending of polymer films? *J. Mater. Chem.*, **18**, 63–65.

37 Choi, H.J., Jeong, K.U., Chien, L.C., and Lee, M.H. (2009) Photochromic 3-dimensional actuator based on an uncrosslinked liquid crystal elastomer. *J. Mater. Chem.*, **19**, 7124–7129.

38 Naka, Y., Mamiya, J., Shishido, A., Washio, M., and Ikeda, T. (2011) Direct fabrication of photomobile polymer materials with an adhesive-free bilayer structure by electron-beam irradiation. *J. Mater. Chem.*, **21**, 1681–1683.

39 Yoshino, T., Kondo, M., Mamiya, J., Kinoshita, M., Yu, Y.L., and Ikeda, T. (2010) Three-dimensional photomobility of crosslinked azobenzene liquid-crystalline polymer fibers. *Adv. Mater.*, **22**, 1361–1363.

40 Fang, L.J., Zhang, H.T., Li, Z.D., Zhang, Y., Zhang, Y.Y., and Zhang, H.Q. (2013) Synthesis of reactive azobenzene main-chain liquid crystalline polymers via Michael addition polymerization and photomechanical effects of their supramolecular hydrogen-bonded fibers. *Macromolecules*, **46**, 7650–7660.

41 Wang, W., Sun, X.M., Wu, W., Peng, H.S., and Yu, Y.L. (2012) Photoinduced deformation of crosslinked liquid-crystalline polymer film oriented by a highly aligned carbon nanotube sheet. *Angew. Chem. Int. Ed.*, **51**, 4644–4647.

42 Harris, K.D., Cuypers, R., Scheibe, P., van Oosten, C.L., Bastiaansen, C.W.M., Lub, J., and Broer, D.J. (2005) Large amplitude light-induced motion in high elastic modulus polymer actuators. *J. Mater. Chem.*, **15**, 5043–5048.

43 Iamsaard, S., Asshoff, S.J., Matt, B., Kudernac, T., Cornelissen, J.J.L.M., Fletcher, S.P., and Katsonis, N. (2014) Conversion of light into macroscopic helical motion. *Nat. Chem.*, **6**, 229–235.

44 Kondo, M., Yu, Y.L., and Ikeda, T. (2006) How does the initial alignment of mesogens affect the photoinduced bending behavior of liquid-crystalline elastomers? *Angew. Chem. Int. Ed.*, **45**, 1378–1382.

45 Kondo, M., Mamiya, J., Kinoshita, M., Ikeda, T., and Yu, Y.L. (2007) Photoinduced deformation behavior of crosslinked azobenzene liquid-crystalline polymer films with unimorph and bimorph structure. *Mol. Cryst. Liq. Cryst.*, **478**, 1001–1013.

46 Yu, Y.L., Nakano, M., Shishido, A., Shiono, T., and Ikeda, T. (2004) Effect of cross-linking density on photoinduced bending behavior of oriented liquid-crystalline network films containing azobenzene. *Chem. Mater.*, **16**, 1637–1643.

47 Yu, Y.L., Maeda, T., Mamiya, J., and Ikeda, T. (2007) Photomechanical effects of ferroelectric liquid-crystalline elastomers containing azobenzene chromophores. *Angew. Chem. Int. Ed.*, **46**, 881–883.

48 Chen, B.Q., Kameyama, A., and Nishikubo, T. (1999) New combined liquid crystalline polymers from polyaddition of biphenol diglycidyl ether and trimeric esters. *Macromolecules*, **32**, 6485–6492.

49 Lee, W.K., Kim, K.N., Achard, M.F., and Jin, J.I. (2006) Dimesogenic compounds consisting of cholesterol and fluorinated azobenzene moieties: dependence of liquid crystal properties on spacer length and fluorination of the terminal tail. *J. Mater. Chem.*, **16**, 2289–2297.

50 Zhang, Y.Y., Xu, J.X., Cheng, F.T., Yin, R.Y., Yen, C.C., and Yu, Y.L. (2010) Photoinduced bending behavior of crosslinked liquid-crystalline polymer films with a long spacer. *J. Mater. Chem.*, **20**, 7123–7130.

51 Priimagi, A., Shimamura, A., Kondo, M., Hiraoka, T., Kubo, S., Mamiya, J.I., Kinoshita, M., Ikeda, T., and Shishido, A. (2012) Location of the azobenzene moieties within the cross-linked liquid-crystalline polymers can dictate the direction of photoinduced bending. *ACS Macro Lett.*, **1**, 96–99.

52 Cheng, F.T., Zhang, Y.Y., Yin, R.Y., and Yu, Y.L. (2010) Visible light induced bending and unbending behavior of crosslinked liquid-crystalline polymer films containing azotolane moieties. *J. Mater. Chem.*, **20**, 4888–4896.

53 Yin, R.Y., Xu, W.X., Kondo, M., Yen, C.C., Mamiya, J., Ikeda, T., and Yu, Y.L. (2009) Can sunlight drive the photoinduced bending of polymer films? *J. Mater. Chem.*, **19**, 3141–3143.

54 Wu, W., Yao, L.M., Yang, T.S., Yin, R.Y., Li, F.Y., and Yu, Y.L. (2011) NIR-light-induced deformation of cross-linked liquid-crystal polymers using upconversion nanophosphors. *J. Am. Chem. Soc.*, **133**, 15810–15813.

55 Jiang, Z., Xu, M., Li, F.Y., and Yu, Y.L. (2013) Red-light-controllable liquid-crystal soft actuators via Low-power excited upconversion based on triplet-triplet annihilation. *J. Am. Chem. Soc.*, **135**, 16446–16453.

56 Yamada, M., Kondo, M., Mamiya, J.I., Yu, Y.L., Kinoshita, M., Barrett, C.J., and Ikeda, T. (2008) Photomobile polymer materials: towards light-driven plastic motors. *Angew. Chem. Int. Ed.*, **47**, 4986–4988.

57 Yamada, M., Kondo, M., Miyasato, R., Naka, Y., Mamiya, J., Kinoshita, M., Shishido, A., Yu, Y.L., Barrett, C.J., and Ikeda, T. (2009) Photomobile polymer materials – various three-dimensional movements. *J. Mater. Chem.*, **19**, 60–62.

58 van Oosten, C.L., Bastiaansen, C.W.M., and Broer, D.J. (2009) Printed artificial cilia from liquid-crystal network actuators modularly driven by light. *Nat. Mater.*, **8**, 677–682.

59 Camacho-Lopez, M., Finkelmann, H., Palffy-Muhoray, P., and Shelley, M. (2004) Fast liquid-crystal elastomer swims into the dark. *Nat. Mater.*, **3**, 307–310.

60 Cheng, F.T., Yin, R.Y., Zhang, Y.Y., Yen, C.C., and Yu, Y.L. (2010) Fully plastic microrobots which manipulate objects using only visible light. *Soft Matter*, **6**, 3447–3449.

61 Chen, M.L., Xing, X., Liu, Z., Zhu, Y.T., Liu, H., Yu, Y.L., and Cheng, F.T. (2010) Photodeformable polymer material: towards light-driven micropump applications. *Appl. Phys. A – Mater.*, **100**, 39–43.

62 Chen, M.L., Huang, H.T., Zhu, Y.T., Liu, Z., Xing, X., Cheng, F.T., and Yu, Y.L. (2011) Photodeformable CLCP material: study on photo-activated microvalve applications. *Appl. Phys. A – Mater.*, **102**, 667–672.

63 Li, C., Cheng, F.T., Lv, J.A., Zhao, Y., Liu, M.J., Jiang, L., and Yu, Y.L. (2012) Light-controlled quick switch of adhesion on a micro-arrayed liquid crystal polymer superhydrophobic film. *Soft Matter*, **8**, 3730–3733.

64 Zhan, Y.Y., Zhao, J.Q., Liu, W.D., Yang, B., Wei, J., and Yu, Y.L. (2015) Biomimetic submicroarrayed cross-linked liquid crystal polymer films with different wettability via colloidal lithography. *ACS Appl. Mater. Interfaces*, **7**, 25522–25528.

65 Yan, Z., Ji, X.M., Wu, W., Wei, J., and Yu, Y.L. (2012) Light-switchable behavior of a microarray of azobenzene liquid crystal polymer induced by photodeformation. *Macromol. Rapid Commun.*, **33**, 1362–1367.

66 Zhao, J.Q., Liu, Y.Y., and Yu, Y.L. (2014) Dual-responsive inverse opal films based on a crosslinked liquid crystal polymer containing azobenzene. *J. Mater. Chem. C*, **2**, 10262–10267.

67 Zeng, H., Martella, D., Wasylczyk, P., Cerretti, G., Lavocat, J.C., Ho, C.H., Parmeggiani, C., and Wiersma, D.S. (2014) High-resolution 3D direct laser writing for liquid-crystalline elastomer microstructures. *Adv. Mater.*, **26**, 2319–2322.

68 Zeng, H., Wasylczyk, P., Cerretti, G., Martella, D., Parmeggiani, C., and Wiersma, D.S. (2015) Alignment engineering in liquid crystalline elastomers: free-form microstructures with multiple functionalities. *Appl. Phys. Lett.*, **106**, 111902.

69 Zeng, H., Wasylczyk, P., Parmeggiani, C., Martella, D., Burresi, M., and Wiersma, D.S. (2015) Light-fueled microscopic walkers. *Adv. Mater.*, **27**, 3883–3887.